# Spreading depressions and periinfarct spreading depolarizations in the context of cortical plasticity

Jan A. Jabłonka[1*], Clemens Mehlhorn[2], Maria Sadowska[1], Władysław Średniawa[4,1,3], Łukasz M. Szewczyk[6], Aleksandra Szlachcic [1], Paulina Urban [5,3], Maciej Winiarski[7],

1 Laboratory of Animal Physiology, Faculty of Biology, University of Warsaw, Warsaw, Poland
2 Humboldt-Universität zu Berlin
3 College of Inter-Faculty Individual Studies in Mathematics and Natural Sciences, University of Warsaw, Warsaw, Poland
4 Laboratory of Neuroinformatics, Nencki Institute of Experimental Biology of PAS, Warsaw, Poland
5 Laboratory of Functional and Structural Genomics, Center of New Technologies, University of Warsaw, Warsaw, Poland
6. Laboratory of Molecular Neurobiology, Centre of New Technologies, University of Warsaw, Warsaw, Poland
7 Laboratory of Emotions Neurobiology, Nencki Institute of Experimental Biology, PAS, Warsaw, Poland
*Corresponding Author:
Jan A. Jabłonka, Laboratory of Animal Physiology, Faculty of Biology, University of Warsaw,
ul. Ilji Miecznikowa 1, 02-096 Warsaw, Poland.
Tel: (4822) 55 41 033
E-mail: jaj@biol.uw.edu.pl

**Abstract —** Studies of cortical function-recovery require a comparison between normal and post-stroke conditions that lead to cortical metaplasticity changes. Focal cortical stroke impairs experience-dependent plasticity (ExDP) in the neighboring somatosensory cortex. A stroke usually evokes periinfarct depolarizations (PiDs) – a spreading depression-like waves. Experimentally induced spreading depressions (SDs) affect gene expression and some of these changes persist for at least 30 days. Such changes are not only stroke-specific: migraine patients had prolonged protein changes after a single SD episode during migraine aura. This study investigates whether non-stroke depolarizations like SDs impair cortical ExDP similarly to the stroke.

Rats were subjected to unilateral SDs. ExDP was induced by a month of contralateral partial whiskers deprivation. Cortical activity was mapped by [$^{14}$C]-2-deoxy-D-glucose (2DG) incorporation during stimulation of spared and contralateral homotopic whiskers. Whiskers deprivation after SDs resulted in normal cortical representation enlargement suggesting that SDs and PiDs depolarization have no influence on ExDP cortical map reorganization. The differences hypothetically influencing metaplasticity in rats were verified and compared between the SDs induced by high osmolarity KCl solution and the PiDs following cortical photothrombotic stroke (PtS).

We conclude neither PiDs nor the previously proposed MMP-9, -3, -2 or COX-2 are directly responsible for cortical post-stroke metaplasticity changes. Only the interhemispheric

activity equilibrium was more imbalanced after stroke. Hence, the interhemispheric interactions modified by stroke may be a promising target for future studies of post-stroke ExDP and convalescence. The results support also more global SDs-mediated modifications, that may have some implications for the migraine states interpretation.

***Keywords:*** 2-DG, barrel field, COX-2, MMP-2, MMP-3, MMP-9, periinfarct depolarizations, PiDs, photothrombotic stroke, SD, spreading depression, whiskers deprivation, cortical plasticity.

**Significance Statement**

We demonstrated a line of comparisons of spreading depressions (SDs) and Pt stroke (PtS) with periinfarct depolarizations (PiDs) which shading a light on the brain steady state in both cases: after stroke – the metaplasticity during rehabilitation and after the spreading depressions– like migraine aura in migraineurs. We show that brains are probably for a long time after the SDs episodes not in a healthy, stabilized condition.

The most important conclusion of this paper however, is that not changes of the chosen proteins (MMPs and COX-2) are responsible for experience dependent plasticity (the rearrangement of cortical sensory representation maps) impairment after stroke and that the interhemispheric interactions are most promising reason responsible for the metaplasticity changes.

The global changes in brain functioning accompanying the SDs are similar to those observed after focal PtS with periinfarct depolarizations but are usually more pronounced after the spreading depressions in our experimental models. However, the efficacy of plasticity in barrel field of rats was diminished only after focal cortical stroke in its vicinity, so SDs have no negative impact on cortical experience dependent plasticity and can even have a positive one.

The cortical concentration changes of chosen metalloproteinases (MMP-2, -3, -9) and COX-2 were mostly similar but more pronounced after SDs, yet MMP-9 was selective for SDs in cortical areas which may have some positive supporting impact on synaptic plasticity. COX-2 was the only protein which differed after stroke in BF. COX-2 with MMP-9 were most pronounced after SDs in BF. Slightly visible MMP-3 decrease was noted in the areas of spreading waves initiation. Changes were observed in the thalamus after SDs but not after PiDs. Slight increase of MMP-9 in thalamus was observed in all the operated animals.

We compared also spreading waves of PiDs and SDs amplitude and duration and frequencies of spontaneous oscillations during the depression period. The PiDs amplitude of the depolarization was a bit lower than SDs but no other differences were observed. The interhemispheric activity ratio was the only difference more pronounced after stroke. Hence, the interhemispheric interactions modified by stroke may therefore be a promising target for future studies of post-stroke experience-dependent plasticity and convalescence.

## Introduction /1032

The primary somatosensory cortex of the whiskers — the barrel field (BF) — is a widely accepted model for studying cortical plasticity due to its well-defined somatotopic organization. The whiskers cortical representation easily rearranges in response to sensory input modification. In mice, a cortical representation of a row of whiskers, functionally visualized by 2DG incorporation, enlarge in width by more than 50% when the surrounding whiskers are cut for 7 days (Dietrich et al. 1985; Kaliszewska et al., 2012). In rats, it was 40% after month of cutting (Jabłonka et al., 2007).

This cortical map reorganization involves CaMKII (Calcium/calmodulin-dependent protein kinase II) and requires NMDA (N-methyl-D-aspartate) receptor-dependent induction of long-term potentiation (LTP, Glazewski et al., 2000; Footitt and Newberry, 1998). It is also accompanied by depressions, similar to long-term depressions (LTD), which weaken synaptic connections within the deprived cortex (Drew and Feldman 2009; Li et al., 2009).

*In vivo* studies after SDs showed that potentiation was uncorrelated with meaningful input (Guiou et al., 2005; Piilgaard and Lauritzen, 2009; Faraguna et al., 2010; de Souza et al., 2011). The SDs induced changes in the sensory cortex of rats typical of cortical plasticity and cortical map remodeling (Theriot et al., 2012). After a stroke, synaptic plasticity seemed to be boosted as well (Hagemann et al., 1998).

However, we found that focal stroke strongly moderated the cortical map rearrangement induced by the partial whiskers deprivation (Jabłonka et al., 2012). Therefore, assuming that the molecular and electrophysiological markers of synaptic plasticity are enhanced after stroke while the ExDP symptoms are reduced, the features we should concentrate on are those that might be correlated to rearrangement of dendritic branches and spines (Tailby et al., 2005).

Marik et al (2010) showed that within days after deprivation was initiated, axons on both excitatory and inhibitory neurons in the spared whiskers sensory representation, elongated in the direction of the neighboring cortex deprived of sensory input. MMP-9 was shown to determine spines' thinning and elongation (Michaluk et al., 2011), supporting the cortical map rearrangement in ExDP (Kaliszewska et al., 2012). On the other hand, we showed that

the contralateral hemisphere is involved in spared whiskers representation-widening in 2DG functional brain mapping (Jabłonka, 2012; Jabłonka et al., 2012; Jabłonka et al., 2014).

A considerable body of data demonstrates that a tiny focal brain injury results in alterations within the entire brain (Witte et al., 2000). A focal cortical stroke changes the brain metabolism for at least few months (Jabłonka et al., 2009; Nonose et al., 2018), and the overall activity in the ipsilateral hemisphere decreases for a few days. Following the diaschisis, an almost immediate post-stroke increase of metabolism related to spontaneous activity is observed in the contralateral hemisphere (Andrews 1991; Mohajerani et al., 2011). GABA-ergic inhibition seems to be reduced bilaterally while the NMDA and AMPA-dependent excitability increases in the lesioned hemisphere (Que et al., 1999; Schiene et al., 1996; Redecker et al., 2002). Consequently, cortical inhibition bilaterally decreases while excitability increases (Neumann-Haefelin and Witte, 2000). In the area of the penumbra, the excitability is decreased following enormous excitation that leads to excitotoxicity and spreading PiDs (Heiss, 2011). The PiDs systematically cross the entire hemisphere, activating the glial cells and modifying tissue excitability and metabolism. The growth of contralateral branches was observed as a result of local thermal coagulation lesion (Carmichael and Chesselet 2002).

Our previous studies showed that focal cortical photothrombotic stroke (PtS) in a vicinity of the BF, inhibits the cortical map remodeling in ExDP induced by whiskers deprivation (Cybulska-Kłosowicz et al. 2011; Jabłonka et al., 2007). The inhibition depended on MMPs and COX-2 expression, probably reflecting an inflammatory response (Cybulska-Kłosowicz et al. 2011; Jabłonka et al., 2012). PiDs were considered a major factor inducing the expression of COX-2 (Koistinaho and Chan, 2000; Miettinen et al., 1997). PiDs are caused by uncontrolled glutamate and potassium release in ischemic tissue with prolonged elevation of extracellular $K^+$ concentration and impaired energy-requiring $K^+$ buffering by the astrocytic syncytium (Nedergaard and Hansen 1988; Hossmann, 1996; Dienel and Hertz, 2005). The extracellular $K^+$ seems to be the main trigger for depolarization and accompanying depression of spontaneous activity (Hartings et al., 2017). The same mechanisms leads to SDs which are responsible for migraine aura in intact brains and for the sustained protein expression changes in humans after the migraine states (Charles and Baca

2013). Experimentally induced SDs that are induced by direct $K^+$ application on the dura surface increase COX-2, MMPs and wide protein expression changes in its target hemisphere (Urbach et al. 2006).

In the described experiments on PtSs the BF distant from the infarct core area (1.2 mm B1–3.2 mm B5 at the end of the row) was under the influence of remotely acting factors. Since COX-2 post-stroke synthesis is mainly induced by the PiDs (Koistinaho and Chan 2000), we decided to check if SDs alone can affect plasticity induced by partial whiskers deprivation. We also looked for crucial differences between the SDs induced by dura KCl application and PiDs observed after cortical PtS to look closer the metaplasticity in this two experimental models.

**We therefore compared** (Tab.1)**:**

(**I**) the whiskers cortical representations and

(**II**) the general metabolic activity pattern

**between groups of:**

**a)** intact animals (n=6),

**b)** animals after ExDP induction, followed by cutting of all the whiskers except row B, for one month (**C**, n=6)

**c)** SDs induced by hyperosmolar KCl dura application (**SD**, n=8),

**d)** hyperosmolar NaCl instead of KCl application in sham animals (**SDS**, n=5),

**e)** PiDs induced by focal cortical stroke (**Pt**, n=6).

**That led us to comparison of:**

(**III**) Electrophysiological features (n=6 for each group) and

(**IV**) Proteomic differences among the groups (n>5 in each group).

(The numbers from **I** to **IV** will be used as a reference to the specific experimental schemes related to these goals throughout the text).

Four proteins in the cortex and thalamus were examined: COX-2, MMP-2, MMP-3, and MMP-9 within the groups. Based on prior results, we suspected that proteins distribution may shed a light on previously observed results concerning the post-stroke ExDP reduction (Cybulska-Kłosowicz et al. 2011; Jabłonka et al., 2007; 2012; Meighan et al., 2006; Nagel et al., 2005; Romanic et al., 1998; Urbach et al. 2006; Wang et al., 2008).

## Results /1712

### Histopathological verification (I, II, IIIA)

After SD-like operations

Both the experimental and sham animals had a surface cortical lesion in the brain location where the solution was applied and PtS induced. The lesion induced by high osmolarity solution was 300 um±120 um in depth and diameter on layer IV: for NaCl – 1±0.5 mm; for KCl - 1.5±0.2 mm, and a cortical surface decomposition in layers II/III on the area of diameter for: NaCl – 3.4 ±0.3 mm, KCl – 4.3 ±0.9 mm was localized mainly in the secondary visual cortex (V2M) and concentric surroundings: medially, the retrosplenial agranular cortex (RS) and laterally, the medial primary monocular area (V1M, Urbach et al. 2006, Fig. 1A).

The high osmolarity-induced lesion edge was in a distance of 4 mm±0.4 mm to the B1 barrel (Fig. 4). There were no structural differences in the distance from 0.2±0.1 mm around the edge of the ***sol*** area, nor in remote areas. The group after aCSF application did not have the lesion on the cortical surface showing only a small oedema which was not statistically significant when compared to intact brain deformations (without craniotomy).

After PtS induction

PtS placed in a part of trunk sensory representation had the diameter at the brain surface equal to that seen the layer IV (1.5±0.5 mm) and was slightly smaller in the supragranular area of layers V, VI (1.3 mm±0.2 mm), leaving white matter intact. However, the CO staining showed a decreased level of optical density at a distance of up two 2 mm from the stroke core center (Fig. 4). The volume of the stroke core, where necrotic cells dominate, was 0.8 $mm^3$±0.3 $mm^3$. The lesion edge was at a distance of 1200±208 μm from the B1 barrel (Fig. 4). There were no structural differences in the distance 0.3±0.2 mm in the stroke core and remote areas of the cortex.

### 2-deoxyglucose (2-DG) brain mapping (I, II)

A multi-factor ANOVA analysis for all the groups revealed significant changes after PtS and SDs in the interhemispheric relation of 2-DG cortical incorporation (**II**, $F_{(2.89)}$=5.38,

p=0.006) and cortical row B representation area (**I**, $F_{(2.95)}$=2.77, p=0.001), as well as in row B width (**I**, $F_{(2.09)}$=10.34, p < 0.0001).

**Experience-dependent plasticity (I)**

After one month of unilateral deprivation of all but one row of whiskers, we observed a widening of the non-deprived row cortical representations in all experimental and control groups (Fig. 2 & 3).

In animals with SDs and a focal lesion induced by 3M KCl, the difference between row B representations was the same as in the both **SDS** and **SDC** groups (p<0.05). The mean percentage difference between deprived and non-deprived sites was like that found in the intact control group **C** (42%±18%). In animals with focal PtS the difference was 11%±9%.

The width of the spared row B representation in the deprived hemisphere of the **Pt** animals differed significantly from homologous areas in all the other groups with whiskers deprivation: **SD, C** (p<0.005) and **SDC** (p=0.04). There were no statistically significant differences between SD-operated groups (Tab. 2, Fig. 2, 3; Supp. 1).

**Metabolic correlates of cortical activity (II)**

In the poststroke brains spontaneous activity seemed to have an important impact on cortical map reorganizations (Jabłonka et al. 2009), therefore we examined the activity related metabolic changes with a 2-DG incorporation level. There were no significant differences between the groups regarding the direct comparison of 2DG incorporation in the tested regions, but the relation between the hemispheres differed from each other. There was no statistically significant interhemispheric imbalance in the **C, SDC,** and **SDS** groups.

In control group (**C**), the interhemispheric ratio of 2DG incorporation in the representations of stimulated rows B was 1± 0.1 μCi/g. It was significantly higher than in surrounding non-stimulated cortex (0.89±0.04 μCi/g from the side of BF centre — side of row **C** and 0.81±0.2 μCi/g laterally — from the side of row A, p > 0.0001) and this tendency did not differ between the groups (Tab. 3a).

For all the measured areas, only the **SD** group had significantly lower 2-DG incorporation in layers IV and V/VI in the treated hemisphere, and 8% lower incorporation in the entire

non-stimulated area of the treated hemisphere a month after the SDs episodes. For the rest of SD-like operated rats the interhemispheric relation of 2-DG incorporation level of all measured areas was comparable between and within the groups and differed significantly from that in the **SD** group (p =0.004, Tab. 3b).

The interhemispheric differences of **SD** animals disappeared when we normalized the values relative to the auditory cortex, which was treated as an activated reference area (layer IV: **Au** – by 7 %, p=0.004, row B – 8%, p=0.007, layers V/VI: **Au** – by 5 %, p=0.05, row B – 4%; p=0.01); it had itself the interhemispheric shift by 7 % in layer IV (LH – 1.27±0.16 μCi/g, RH – 1.19±0.11 μCi/g).

One month after the stroke, the post-stroke group (**Pt**) had a shift of interhemispheric relation which was 13% higher in the intact hemisphere (Fig. 5, Tab. 3b) than in the treated one. Both the **Pt** and **SD** groups differed significantly from controls (**SD** p=0.03, **Pt**: p=0.004).

Comparisons of all the groups allow us to combine groups **C, SDC,** and **SDS** to a single super-group with stabilized interhemispheric relation of activity, and to combine groups **SD** with **Pt** to a super-group in which the interhemispheric activity equilibrium was affected. There were no differences within these two super-groups in the interhemispheric ratio, but the difference ratio between them was pronounced (p=7E-05).

**Electrophysiological brain activity (III)**

Looking for other differences between post-stroke and post-spreading depolarization conditions, we examined spontaneous cortical activity from electrocorticograms (ECoGs) recorded for 2h after the beginning of PtS induction (light on) in **Pt** group, and 2h since solution application in **SD** group. The signals were compared to spontaneous activity in **SDC** animals after an aCSF cortical application and shams (**SDS**) with 3M NaCl applied.

*(IIIA).* The ECoG pattern was normal, similar to isoflurane anesthesia in rats (Michelson and Kozai, 2018) when monitoring started. The first depolarization appeared 42±23 [s] in **Pt** and 10±2 [s] in **SD** groups after rose Bengal injection or KCl application, respectively.

The statistically significant different was the duration of the depolarization wave of SDs 92±59 [s] and PiDs 108±39 [s] (F=4.53, p=0.03). Measurements of slow wave [<1Hz]

oscillations showed no significant differences between these groups. SDs and PiDs frequency (SDs: 3.8 ±1.9 Hz, PiDs: 2.9±1.3 Hz) and the amplitude from the baseline (SDs: 0.47±0.2 mV, PiDs: 0.48±0.5 mV) and the area below the depolarization wave were similar. The amplitude, however, was higher in PiDs when we compared it between the minimal and the maximal values within the analyzed period (p=0.042).

During depolarizations, a spreading depressions appeared — a pronounced silencing of the spontaneous oscillations over 3 Hz — in both **Pt** and **SD** animals (Fig. 6). The spectrograms did not reveal any difference between SDs and PiDs in a specific frequency band. In the **SD** group, the silencing of the oscillations exceeded the depolarization some time afterward (Fig. 7). However, there was no significant difference between PiDs and SDs in that respect as well.

*(IIIB).* The multielectrode recordings in **SD** animals allowed us to visualize four types of depolarization waves traversing the space: 1) classical **SD**-like waves when depolarizations appeared on three or more adjacent electrodes in a radial epicentral direction from ***sol,*** the source of K+ ions in the 3 M KCl application site; 2) presumed SD-like waves with sequential onset at 2 adjacent recording sites; 3) reversed SD-like waves (rSD) with the spreading sequence between electrodes reverse to the initial one and 4) non-spreading transient depolarizations with ECoG amplitude reduction below 50% on some electrodes, without clear evidence of propagation between them or inconsistent spreading plan (Fig. 8, Supp. Fig. 2). There were no differences between the shape of the amplitude or the time duration between the waves.

**Protein expression analysis by Western blot**

The ExDP results we obtained were unexpected; we therefore hypothesized that the observed similarities in the protein regulation after SDs and PiDs may be not so similar as the results reported in the literature and data metanalysis suggested. However, since there were no previous proteomic experiments performed simultaneously on both post-SDs and post-PiDs brain tissues, we analyzed proteins changes in both our experimental models using a comparative western blot paradigm. The chose proteins that were shown in previous studies to influence deprivation-induced cortical representation maps rearrangement: COX-2 and

MMPs (MMP-2, MMP-3, MMP-9; Cybulska-Kłosowicz et al., 2011; Jabłonka et al., 2012; Urbach et al., 2006).

In **C** animals, COX-2 and MMP-3 had a basal level of cortical expression. MMP-2 and MMP-9 in the cortex of **C** animals were barely observed in the somatosensory areas, and in most cases were not present at all. The COX-2 concentration was higher in all experimental groups, but was highest in **SD** somatosensory areas. In ***BF*** of the SD-operated animals, significant increase of all monitored proteins was observed; this was different from the **Pt** group, which showed only COX-2 increase. In the **SD** group, only COX-2 and MMP-9 increases exceeded the level observed in sham animals. The level of MMP-3 in ***BF*** increased in all the SD-like operated animals but in other cortical regions it increased only in the **SDS** group. In all monitored cortical areas MMP-9 increase was most pronounced in **SD** animals.

Regarding the thalamic proteins concentration (***Th***), COX-2 and MMP-9 were absent in **C** animals but MMP-2 and -3 had a basal level of expression. MMP-2, -9 and COX-2 appeared in the thalami of all experimental groups. However, the increase was significant only for MMP-2 in the thalami after SDs performed in the cortex a day before. MMP-3 slightly decreased in **SD** and **SDS** animals, but again, not significantly. In almost all the areas the **SD** group seemed to be the most strongly affected.

The differences between the groups resulted in different gel migration of some undefined bands recognized by antibodies. We assumed that by following them, we may gain valuable information about the mechanisms underlying these proteins activities, believing that future analysis and further proteomic works will allow one to understand the described differences. The cortical modifications of the additional bands, which appeared repeatedly in different areas were reported for each protein band and are described in detail in the supplementary material.

## Discussion /3546

In this paper we examined the post-SDs and post-stroke cortical plasticity *in vivo* by eliciting partial sensory deprivation of the barrel cortex. In healthy rodents, leads to enlargement of the cortical representation of the spared whiskers at the expense of the surrounding area (Glazewski and Fox, 1996). The pronounced alterations of brain activity following small ischemic injuries affect many aspects of cortical plasticity, including an

increase in LTP propensity around the ischemic lesion (Hagemann et al., 1998; Mittmann and Eysel, 2000) and an enhancement in seemingly meaningless synaptic connectivity that is independent of any purposeful stimulation (Calabresi et al., 2003). Meanwhile, the ischemia increases expression of proteins from the signaling pathways inhibitory to axonal outgrowth like the myelin-associated proteins (Li et al., 2010) or ephrins (Overman et al., 2012).

Our findings confirm that cortical focal stroke lowers ExDP efficiency. In the BF vicinity, the PtS widened the cortical representation of the spared whiskers sensory input surrounded by the deprived cortex (when visualized by 2DG incorporation during bilateral stimulation of spared and homotopic contralateral rows of whiskers). Previous research showed partial restoration of this plasticity impairment when the deprivation onset is delayed after the PtS induction (Jabłonka et al., 2009).

The present results show SDs (induced by the occipital cortex exposition to highly osmotic KCl solution followed by a month of unilateral partial whiskers deprivation) did not influence the expansion of spared whiskers cortical representation. Neither the small cortical surface lesion in the occipital cortex nor the SD waves influenced the ExDP in the sensory whiskers representation. What, then, makes these two similar phenomena (SDs and PiDs) so different in respect of metaplasticity changes?

## Alternative mechanisms that might trigger stroke-induced decrease in cortical plasticity

PtS in the barrel cortex vicinity inhibit plasticity in a COX/PPARs and MMPs dependent manner (Jabłonka et al., 2012; Cybulska-Kłosowicz et al., 2011). The accompanying PiDs are the main factor influencing the post-stroke increase of COX-2 tissue concentration or PPARs activation (Miettinen et al., 1997; Ou et al., 2006; Victor et al., 2006) and subsequent MMPs transcription modifications in the ischemic hemisphere (Candelario-Jalil et al., 2007; Kriz and Lalancette-Hébert 2009). However, we found that the SDs depolarization waves did not change the vulnerability to ExDP cortical map reorganization. We therefore had to consider other factors which could underlie ExDP vulnerability.

### Post injury situations

Range of lesions

Both **SD** and **Pt** animals had lesions, but their origin, shape, and range were different. **SD** animals had a surface cortical lesion in the occipital cortex, while **Pt** animals had a columnar lesion in the somatosensory area across all the white matter layers (Jabłonka et al., 2009, 2012).

Song and Yu (2013) found that PiDs accompany the PtS, while SDs induce cells shrinkage in the highly osmotic KCl solution and swelling in the surrounding area leading to the cortical surface injury. The highly osmotic NaCl solution did not induce depolarizations in SD-operated sham animals (SDS), but produces one-third size lesion compared to those observed in the **SD** group. Although impossible to confirm directly, the highly osmotic solutions are expected to cause cellular shrinkage and cell death, but unlike the case for **SD** animals, the surrounding swelling episodes do not accelerate additional lesion enlargement (as does treatment with KCl). Therefore, a larger lesion size in **SD** vs. **SDS** animals could be treated as a depolarization-induced cell death in the uncomfortable conditions of non-optimal osmotic pressure. Conversely, Pt lesions are induced by regional blood supply restriction, and energetic and metabolic cells failure accompanies PiDs, enlarging the stroke core size by 30% (Song & Yu, 2013). SDs lesion destroyed layers II/III of the secondary visual cortex, while the entire cortical columns were destroyed by PtS in a part of the trunk's sensory representation (Fig 1B, 4B).

The distance between the lesions edge and the B1 barrel in **SD** doubled the **Pt** distance. PtS experiments demonstrate that the affected Pt lesion core area is more restricted than in other stroke models. Pt is assumed not to induce penumbra effect (Sommer, 2017), spreading the lesion affected area on the territories wider than the blood flow reduction. Therefore, none of the lesions in our experiment should directly affect the ***BF*.**

### Cortical activity

Spontaneous cortical activity, monitored through electrophysiological recordings and metabolic changes, synchronizes widespread areas and regulates neurites growth. Despite some similarities, the electrophysiological and metabolic modifications after PiDs and SDs have different impact on cortical activity homeostasis and/or on interregional wiring.

SDs require high energy supply, and during SD episode in awake animals, one of largest known cortical 2-DG incorporation occurs (Shinohara et al., 1979). In the post-SDs phases, rapid cerebral blood flow (CBF) increases, followed by a prolonged and sustained CBF decrease (Fabricius et al., 1995).

Our previous work on rats showed a long-term bilateral metabolic activity changes after PtS visualized by 2DG incorporation. External stimulation never influenced the metabolic correlates of the cortical activity modified by the injury present for at least a month, and stabilizing two months after stroke (Jabłonka et al., 2009). The activity of hemisphere contralateral to the injury, inhibitory to injured hemisphere was documented (Butefisch et al. 2003). Therefore, the upraise of the metabolic activity may underlie the interhemispheric inhibition, hypothetically reducing the plasticity changes that follow the stroke. We hypothesized that the cortex wiring changed and that the metaplasticity was altered under these conditions, in line with Carmichael and Chesselet (2002) findings. These authors found that some experimentally induced focal cortical lesions can support the neurites growth and defined their direction when the frequency of target area oscillations rhythm was 0.1-0.4Hz. We found no differences between the groups regarding the ECoG signals neither in this nor in the other frequencies (Fig. 7 & 8). However, Carmichael and Chesselet's (2002) observed oscillations a few days after the induction of the lesion within areas functionally connected to the lesion area, so that may still require further consideration.

Unlike Jabłonka et al. (2007), we compared also the post-stroke and post-SDs metabolic activity by measuring 2-DG incorporation in more defined cortical areas one month after the induced episodes. The detected difference in non-stimulated cortical areas disappeared upon comparing the activity relative to the excluded stimulated area of auditory cortex (***Au***), suggesting that just as after Pt stroke, the spread 2DG an incorporation increase after SD was related to energy-requiring spontaneous activity or physiological metabolic changes more than to stimulation-related electrophysiological activity. The interhemispheric differences disappeared in that comparison as well. This means we observed non-stimulation related interhemispheric changes in metabolic activity a month after the SDs and PiDs episodes. Therefore, we may confirm the widely described interhemispheric activity changes after stroke are related to PiDs.

To determine and compare the amplitude and frequency of the depolarizing waves (SDs and PiDs) crossing BF, we used single electrode recordings, which demonstrated the spreading waves similarity with a bit higher amplitude of SDs. The multielectrode prefrontal cortex recordings showed radial flow from the core locus of the treatment after applying KCl solution onto the occipital area. However, reversed and irregular waves without a defined trajectory were also observed, in line with recent evidence (Kaufmann et al., 2016) that showed less SDs homogeneity than previously described. That may require a more closer verification with ECoG recordings of the BF, especially that not only the SDs propagation variety was described within the cortex but also some basic features that indicate the special vulnerability of the barrel cortex to SD generation when the extracellular potassium concentration increases (Bogdanov et al. 2016).

**Proteins**

Why does not SD inflammatory induction inhibit plasticity (Jander et al., 2001), while the post-stroke COX-2/PPARs and/or MMPs induction does (Cybulska-Kłosowicz, 2011)? SDs/PiDs were assumed to be mainly responsible for transcription changes in areas "remote from" the cortical injury locus (Hermann et al., 1999; Küry et al., 2007; Miettinen et al., 1997). In our experiments the stroke-induced lesion edge distance from the closest B1 barrel edge was 1.2 mm. The furthest barrel of the non-deprived row B was almost 3 mm away, which is typically described as the "remote non-ischemic cortex" (Küry et al., 2004).

The PiDs-related changes of the protein expression profile after focal stroke in the remote areas of the affected hemisphere and the changes accompanying SDs were very similar (Cybulska-Kłosowicz, 2011; Gursoy-Ozdemir et al., 2004; Urbach et al., 2006). However, no experiments described this similarity in the same experimental set up, comparing the same blots. There were no comparisons of the spatial expression profiles between these two cases. We therefore separately compared some chosen cortical regions that were either closer or more distant from the treated areas and the thalamus.

Previous reports showed that SDs induce additional COX-2 synthesis in the whole hemisphere at least up to the 5th day (Dihné et al., 2002; Horiguchi et al., 2006; Nedergaard and Hansen, 1988; Urbach et al., 2006), and MMP-9 overexpression was also demonstrated a few days after SDs (Gursoy-Ozdemir et al., 2004). In migraine patients, however, the

plasma MMP-9 increase was independent of the detected migraine aura, which is presumed to be caused by SDs episodes, so its simple relation to SDs might be challenged (Ayata 2010; Charles and Baca, 2013; Imamura et al., 2008; Theriot et al., 2012).

Caused by the PiDs (Koistinaho and Chan, 2000) up-regulation of post-stroke COX-2 expression leads to MMP-9 induction which may directly digest PPARs (Itatsu et al., 2009; Xue et al., 2010). Nevertheless, PPARs were also up-regulated after stroke (Ou et al., 2006; Victor et al., 2006). PPAR-gamma inhibits MMP-9 expression (Lee et al., 2010; Yin et al., 2010) but it is still insufficient during stroke as its expression is greatly increased after MCAO (Fukuda et al., 2004). The proteins concentration, however, might be elevated differently in various regions to reach different equilibria with different features for metaplasticity.

Some of the studies concerning spreading depolarizations deal with ischemic injury (Anderson et al., 2003; Chapuisat et al., 2008; Dreier, 2011). Since post-stroke and post-SDs changes are characterized by similar dynamics of proteins changes (Gursoy-Ozdemir et al., 2004; Jabłonka et al., 2012) and the participation of some of the proteins were described in dendrites, spines, and synapses remodeling and therefore cortical plasticity mechanisms (Ethell and Ethell, 2007; Fujioka et al., 2012), we decided to examine the presence of MMP-2, -3, -9, and COX-2 after SDs and PiDs. These proteins were chosen because previous results showed a restoration of deprivation-induced plasticity in BF after PtS following i.p. injections of FN-439 (MMPs inhibitor) or ibuprofen (unspecific COXs inhibitor and PPARs activator; Cybulska-Kłosowicz, 2011; Jabłonka et al., 2009, 2012).

Contrary to other tissues, the brain's COX-2 is constitutively expressed but both constitutive and inducible pools participate in synaptic plasticity and facilitate electrophysiological and behavioral symptoms of cognitive functions (Sang and Chen, 2006). The matrix metalloproteinases, including MMP-2, MMP-3, and MMP-9, are synthesized and secreted as inactive proenzymes (zymogen), which are enzyme-activated in the extracellular space through different MMPs domain interactions (Djuric and Zivkovic, 2017; Woessner, 1991). We observed antibody recognizable, group-specific additional bands for MMPs (Supp. Fig 9-2); we assumed that each "additional band" can be a marker of different proteinases function. (Phillips et al., 2014).

The cortical synthesis of MMP-3 and COX-2 in the **C** group (Fig. 9 & 10; Supp. Fig. 5), confirm the constitutive expression of these two proteins in rats as it was described for human brains (Kirkby et al., 2016), since both participate in the establishment of cortical plasticity. Yet, MMP-2 and MMP-9 were undetected in none of the selected **C** areas. However, since MMP-9 were expressed at low level within the healthy brain synapses (Huntley, 2012; Reinhard et al., 2015), it was probably below our Western Blot detection threshold (as previously shown in mice; see Wang et al., 2000).

In the thalamus (***th***) of mice, COX-2 mRNA and MMP-9 protein and its activity were undetected (Samad et al., 2001; Wang et al., 2000) and this is also confirmed in this study. However, we have shown constitutive expression of the active form of MMP-2 (64kDa) and MMP-3 (53kDa) in the ***th*** of the **C** group.

*Post-stroke and post-SDs protein changes*

Although COX-2, MMPs, and PPARs influence the lesion size (Gu et al., 2005), no changes in the infarct core volume were observed after ibuprofen or FN-439 treatment in our focal photothrombotic stroke model (Cybulska-Kłosowicz, 2011; Jabłonka et al., 2009, 2012). Therefore, it is improbable that COX-2 or MMPs inhibition or PPAR-gamma induction reduced the lesion-induced necrosis size. This suggests that direct cells necrosis in the infarct core does not influence plasticity after stroke. COX-2 was the only protein in ***BF*** whose concentration was increased following PtS with PiDs. Our results also demonstrate the MMP-9 is not the most strongly activated metalloproteinase after focal cortical stroke. In ***BF***, it was detected only after SDs and had much lower expression than MMP-2 and -3, which both were up-regulated by high molarity solution applications. In the stroke core region, MMP-3 decreased while MMP-2 which tended to be synthesized due to the injury, did not.

Anja Urbach et al. (2006) results showed 1.6-fold increase in COX-2 mRNA in the somatosensory cortex 24h after SDs induction by KCl. This increased expression persisted at this level until the 7th day. Other studies also detected increased COX-2 protein up-regulation within 24h (Bidmon et al., 2000; Koistinaho et al., 1999; Thomson and Hakim, 2005). Hence, there are similarities in the COX-2 increase following Pt focal lesion and SD.

However, the present study shows that SDs are much stronger COX-2 synthesis boosters than PtS.

**C** animals exhibit a relatively similar level of the cortex constitutive COX-2 expression in all monitored areas (~150 [An]). In the ***BF*** of the **SD** group, the concentration of COX-2 was increased by 5.3 and in **Pt** by 3.2 (Fig 9). There was, however, cross-correlation between ***sol*** and ***s*** places in these groups. Both had the lowest COX-2 increase in the cortex of the affected areas (**Pt** in ***s*** and **SD** in ***sol***). This suggests that COX-2 upregulation is more strongly related to intact tissue after stroke than directly to the injured areas where MMP-2 prevails.

The cortical basal interregional comparisons for COX-2 have relatively low deviations (**C**: 165±5; SDS: 435±76; **SD**: 843±30, **Pt**: 448±02), constituting 11% when expressed as a mean percentage interregional deviation (PD). Regarding the cortical areas, the amount of COX-2 increase was the same in the areas closer and more distant from the source of spreading waves (Supp Tab. 1). This was unlike metalloproteinases, which showed high interregional deviations (MMP-2 and -3: 72%, MMP-9: 107%). This is unlikely to be a methodological artefact since the results were repeated in several different setups. Future studies should establish whether the differences are related to some yet undescribed features of MMPs dynamics during post-injury reorganization.

MMP-2 zymogen (72kDa) was present mainly in the treated animals and the bands were most prominent in ***s*** of **SDS** and **SD** animals. In ***BF***, the MMP-2 bands were only present in the active form of 64kDa. **SD** and **SDS** groups had the strongest bands of the active form of MMP-2 and were interestingly most pronounced in ***BF***, although the closest area had a lower level of the active form of MMP-2 and even less than the zymogen, which was three times lower than in ***BF*.** In ***sol,*** MMP-2 bands in **SDS** and **Pt** were visible but similar within groups (PD=1.5%). The most pronounced MMP-2 activation can be seen in the ***BF*** of **SDS** animals. Thus, the solution application and the subsequent ions equilibrium changes may have triggered MMP-2 zymogen synthesis and its high-level activation in the ***BF*** but not necessarily in the surrounding cortex which might be less vulnerable to the extracellular ion changes (Bogdanov et al. 2016). Only two animals of the **Pt** group had pro-MMP-2 (64kDa) in BF, but the bands were relatively pronounced (~ 300 [An]). This could be a result of ion diffusion and/or the time-dependent difference between stroked animals. Again, the cross-

correlation was visible between the treated areas (***s*** & ***sol***) so the **Pt** group had the bands less visible in the ***s*** area and **SD** in the ***sol*** area. MMP-9 was increased in all the six **SD** animals mostly in the ***sol*** area. However, four of them showed highly enhanced expression of MMP-9 (~400 [An]). In two other animals the bands were barely detectable in ***s*** (~20 [An]). Nevertheless, the SD group was the only one which had MMP-9 concentration increased in all the cortical areas, which may support the experience-dependent plasticity in the cortex affected by the SDs (Kaliszewska et al. 2011).

MMP-3 was the only metalloproteinase whose 45kDa full-length domain was present in **C** animals in all the cortical areas. Its level was relatively stable across the cortex (around 400 [An], PD=1.5%). Unfortunately, the ***s*** region (**C**: 131 [An]), its exposition time being reduced could not be compared with other areas. Contrary to both previous MMPs, the MMP-3 level diminished in the injured cortical regions (***s*** in **Pt**, ***sol*** in **SD** & **SDS**) and in the other areas increased or remained unchanged for animals treated with osmotic solution and after stroke, respectively.

Diverse forms of metalloproteinases might require consideration since the unspecific MMP-s inhibition is effective in partial post-stroke ExDP restoration (Cybulska-Kłosowicz, 2011). Probably a free-floating MMP-9 was observed in post-SDs animals. However, we cannot say now what could be the role of transmembrane forms (Itoh 2015) in the metaplasticity establishment, although their role might be important as well (Monea 2006).

Thalamic changes in all groups were less pronounced, and COX-2 (bands 72 kDa) were not observed. However, an epitope on bands around 180kDa was detected in **C**, **Pt** and two **SDS** (Supp.2). MMP-2 was not detected in the intact **C** animals neither in the thalamus nor in the cortex. (Supp.3).

In the thalamus, as in the cortex, the full-length MMP-3 showed a 45 [An] band. MMP-9 in the **C** animals were undetected in the thalamus and the cortex. In the thalamus MMP-9 was only present in one **SDS** animal (Supp.4) However, additional epitope of 26kDa bands of MMP-9 was present in the thalamus of all experimental groups but not the controls. The epitope was detected just in the thalamic probes, suggesting a different damage mechanism from that observed in the cortex or even the thalamic MMP-9 specific function. Thus, it is not only stroke that induces thalamic changes through retrograde signaling or even cell death.

The SDs too can modify the thalamic functioning involving the metalloproteinases and COX-2 changes.

Comparison of SDs and focal stroke with PiDs influence on protein expression shows no obvious relation between COX-2, MMP-2, -3 (Supp. 5) and -9 and ExDP. This suggests that higher protein levels in the ***BF*** are not the factor inhibiting the widening (visualized by 2DG), of the spared whiskers representation after stroke, as all the changes were at least doubled in the **SD** group which had no influence on ExDP. The SDs seemed to have the strongest influence on prominent cortical protein up-regulation and induced changes in the thalamus as well (the increase of MMP-2, and MMP-9 (epitope 26kDa) and atypical epitopes of COX-2 (180kDa)).

Interestingly, the two of the three animals which had MMP-2 in ***th*** had also increased active form of MMP-2 (64kDa) concentration in the cortex's ***BF*** region. This suggests the MMP-2 activity is vulnerable to focal cortical stroke influences. It is in line with results showing MMP-2 increase, extracellular transfer and colocalization with GAP-43 in an area with anterograde connections from injured cochlea (Fredrich and Illing 2009). Gontier et al (2009) suggested that MMP-2 enables synaptogenesis to the GAP-43 but it may also release neurites from extracellular semaforins and reinforce the dendritic trees rearrangement. Therefore, MMP-2 "the major actor in extracellular matrix recomposition" should support the cortical map remodeling in ExDP. The lower metalloproteinases concentration in the **SD** groups (compared to the **Pt** group) could explain the observed changes in metaplasticity, although not for the control animals which always had the lowest concentration of metalloproteinases. This suggests an existence of competitive mechanisms which balance and compensate the plasticity-supporting changes in post-injury tissue rearrangement.

**Concluding remarks**

The most important conclusion of this paper is that not the chosen proteins changes are responsible for experience dependent plasticity impairment after focal cortical stroke. The global changes in brain functioning accompanying the spreading depressions are similar to those observed after focal Pt lesion with periinfarct depolarizations. In a meantime, the efficacy of plasticity in BF was diminished only after focal cortical stroke in its vicinity, so

SDs have no negative influence on cortical experience dependent plasticity but can have a positive one via MMP-9 upregulation.

The results also show that the spreading depressions considered responsible for migraine aura had a global influence on the brain functioning and induce not only the protein expression changes in entire depolarized hemisphere but also in thalamus. Pronounced dysregulation in cortical activity and interhemispheric activity equilibrium was observed even a month after the speeding depression episodes.

The cortical concentration changes of chosen metalloproteinases (MMP-2, -3, -9) and COX-2 were mostly similar after PtS and SDs but more pronounced after SDs, yet MMP-9 was selective for SDs in cortical areas. COX-2 was the only protein which increased in BF one day after stroke in its vicinity. COX-2 and MMP-9 increase in BF were most pronounced after SDs. Slight decrease of MMP-3 was noted in the injured areas of spreading waves initiation. Changes were observed in the thalamus after SDs but not after PiDs one day after. Slight increase of MMP-9 in thalamus was observed in all the animals with focal injury in the cortex which might suggest a kind of thalamic reorganization.

The PiDs amplitude of the depolarization was a bit lower than SDs but no other differences were observed in duration and frequencies of spontaneous oscillations during the depression period. The spreading waves of SDs had no radial distribution within the cortex which suggest it is spreading diversely within the cortical areas.

Although the changes observed in our experimental models are usually more pronounced after SDs, the interhemispheric activity ratio was an exception, and was higher after stroke. Hence, the interhemispheric interactions modified by stroke may therefore be a promising target for future studies of post-stroke experience-dependent plasticity and convalescence.

## References


Anderson MF, Blomstrand F, Blomstrand **C,** Eriksson PS, Nilsson M. Astrocytes and stroke: networking for survival? Neurochemical research. 2003 Feb 1; 28(2):293-305.

Andrews RJ. Transhemispheric diaschisis. A review and comment. Stroke. 1991 Jul; 22(7):943-9.

Ayata C. Cortical spreading depression triggers migraine attack: pro. Headache: The Journal of Head and Face Pain. 2010 Apr; 50(4):725-30.

Butefisch CM, Netz J, Wessling M, Seitz RJ, Homberg V. Remote changes in cortical excitability after stroke. Brain 2003; Mar; (3)126:470–81.

Bidmon HJ, Oermann E, Schiene K, Schmitt M, Kato K, Asayama K, Witte OW, Zilles K. Unilateral upregulation of cyclooxygenase-2 following cerebral, cortical photothrombosis in the rat: suppression by MK-801 and co-distribution with enzymes involved in the oxidative stress cascade. Journal of chemical neuroanatomy. 2000 Nov 1; 20(2):163-76.

Bogdanov VB, Middleton NA, Theriot JJ, Parker PD, Abdullah OM, Ju YS, Hartings JA, Brennan KC. Susceptibility of primary sensory cortex to spreading depolarizations. Journal of Neuroscience. 2016 Apr 27; 36(17):4733-43.

Calabresi P, Centonze D, Pisani A, Cupini LM, Bernardi G. Synaptic plasticity in the ischaemic brain. The Lancet Neurology. 2003 Oct 1;2(10):622-9.

Candelario-Jalil E, González-Falcón A, García-Cabrera M, León OS, Fiebich BL. Post-ischaemic treatment with the cyclooxygenase-2 inhibitor nimesulide reduces blood–brain barrier disruption and leukocyte infiltration following transient focal cerebral ischaemia in rats. Journal of neurochemistry. 2007 Feb;100(4):1108-20.

Carmichael ST, Chesselet MF. Synchronous neuronal activity is a signal for axonal sprouting after cortical lesions in the adult. Journal of Neuroscience. 2002 Jul 15;22(14):6062-70.

Chang JC, Shook LL, Biag J, Nguyen EN, Toga AW, Charles AC, Brennan KC. Biphasic direct current shift, haemoglobin desaturation and neurovascular uncoupling in cortical spreading depression. Brain. 2010 Mar 25;133(4):996-1012.

Chapuisat G, Dronne MA, Grenier E, Hommel M, Gilquin H, Boissel JP. A global phenomenological model of ischemic stroke with stress on spreading depressions. Progress in biophysics and molecular biology. 2008 May 1;97(1):4-27.

Charles AC, Baca SM. Cortical spreading depression and migraine. Nature Reviews Neurology. 2013 Nov;9(11):637.

Conant K, Gottschall PE. Matrix metalloproteinases in the central nervous system. Imperial College Press; 2005 Jan 1.

Cybulska-Kłosowicz A, Liguz-Lecznar M, Nowicka D, Ziemka-Nalecz M, Kossut M, Skangiel-Kramska J. Matrix metalloproteinase inhibition counteracts impairment of cortical experience-dependent plasticity after photothrombotic stroke. European Journal of Neuroscience. 2011 Jun;33(12):2238-46.

de Souza TK, e Silva MB, Gomes AR, de Oliveira HM, Moraes RB, de Freitas Barbosa CT, Guedes RC. Potentiation of spontaneous and evoked cortical electrical activity after spreading depression: in vivo analysis in well-nourished and malnourished rats. Experimental brain research. 2011 Oct 1;214(3):463-9.

Dienel GA, Hertz L. Astrocytic contributions to bioenergetics of cerebral ischemia. Glia. 2005 Jun;50(4):362-88.

Dietrich WD, Ginsberg MD, Busto R, Smith DW. Metabolic alterations in rat somatosensory cortex following unilateral vibrissal removal. Journal of Neuroscience. 1985 Apr 1;5(4):874-80.

Dihné M, Grommes **C,** Lutzenburg M, Witte OW, Block F. Different mechanisms of secondary neuronal damage in thalamic nuclei after focal cerebral ischemia in rats. Stroke. 2002 Dec 1;33(12):3006-11.

Djuric T, Zivkovic M. Overview of MMP Biology and Gene Associations in Human Diseases. The Role of Matrix Metalloproteinase in Human Body Pathologies. 2017 Dec 20:1.

Dreier JP. The role of spreading depression, spreading depolarization and spreading ischemia in neurological disease. Nature medicine. 2011 Apr;17(4):439.

Drew PJ, Feldman DE. Intrinsic signal imaging of deprivation-induced contraction of whisker representations in rat somatosensory cortex. Cerebral Cortex. 2008 May 30;19(2):331-48.

Ethell IM, Ethell DW. Matrix metalloproteinases in brain development and remodeling: synaptic functions and targets. Journal of neuroscience research. 2007 Oct;85(13):2813-23.

Fabricius MA, Akgoren NU, Lauritzen M. Arginine-nitric oxide pathway and cerebrovascular regulation in cortical spreading depression. American Journal of Physiology-Heart and Circulatory Physiology. 1995 Jul 1;269(1):H23-9.

Faraguna U, Nelson A, Vyazovskiy VV, Cirelli **C,** Tononi G. Unilateral cortical spreading depression affects sleep need and induces molecular and electrophysiological signs of synaptic potentiation in vivo. Cerebral Cortex. 2010 Mar 26;20(12):2939-47.

Footitt DR, Newberry NR. Cortical spreading depression induces an LTP-like effect in rat neocortex in vitro. Brain research. 1998 Jan 19;781(1-2):339-42.

Fredrich M and Illing RB. MMP-2 is involved in synaptic remodeling after cochlear lesion. Regeneration and transplantation. NeuroReport. 2010 Nov 21:324–327

Fujioka H, Dairyo Y, Yasunaga KI, Emoto K. Neural functions of matrix metalloproteinases: plasticity, neurogenesis, and disease. Biochemistry research international. 2012;2012.

Fukuda S, Fini CA, Mabuchi T, Koziol JA, Eggleston Jr LL, del Zoppo GJ. Focal cerebral ischemia induces active proteases that degrade microvascular matrix. Stroke. 2004 Apr 1;35(4):998-1004.

Glazewski ST, Fox KE. Time course of experience-dependent synaptic potentiation and depression in barrel cortex of adolescent rats. Journal of neurophysiology. 1996 Apr 1;75(4):1714-29.

Glazewski S, Giese KP, Silva A, Fox K. The role of α-CaMKII autophosphorylation in neocortical experience-dependent plasticity. Nature neuroscience. 2000 Sep;3(9):911-8.

Gonthier B, Koncina E, Satkauskas S, Perraut M, Roussel G, Aunis d, Kapfhammer JP0, Bagnard D. A PKC-Dependent Recruitment of MMP-2 Controls Semaphorin-3A Growth-Promoting Effect in Cortical Dendrites. 2009 PLoS One. 2009; 4(4): e5099.

A PKC-Dependent Recruitment of MMP-2 Controls Semaphorin-3A Growth-Promoting Effect in Cortical Dendrites

Gu Z, Cui J, Brown S, Fridman R, Mobashery S, Strongin AY, Lipton SA. A highly specific inhibitor of matrix metalloproteinase-9 rescues laminin from proteolysis and neurons from apoptosis in transient focal cerebral ischemia. Journal of Neuroscience. 2005 Jul 6;25(27):6401-8.

Guoiu M, Sheth S, Nemoto M, Walker M, Pouratian N, Ba A, Toga AW. Cortical spreading depression produces long-term disruption of activity-related changes in cerebral blood volume and neurovascular coupling. Journal of biomedical optics. 2005 Jan;10(1):011004.

Gursoy-Ozdemir Y, Qiu J, Matsuoka N, Bolay H, Bermpohl D, Jin H, Wang X, Rosenberg GA, Lo EH, Moskowitz MA. Cortical spreading depression activates and upregulates MMP-9. The Journal of clinical investigation. 2004 May 15;113(10):1447-55.

Hagemann G, Redecker **C,** Neumann-Haefelin T, Freund HJ, Witte OW. Increased long-term potentiation in the surround of experimentally induced focal cortical infarction. Annals of Neurology: Official Journal of the American Neurological Association and the Child Neurology Society. 1998 Aug;44(2):255-8.

Hartings JA, Shuttleworth CW, Kirov SA, Ayata **C,** Hinzman JM, Foreman B, Andrew RD, Boutelle MG, Brennan KC, Carlson AP, Dahlem MA. The continuum of spreading depolarizations in acute cortical lesion development: examining Leao's legacy. Journal of Cerebral Blood Flow & Metabolism. 2017 May;37(5):1571-94.

Heiss WD. The ischemic penumbra: correlates in imaging and implications for treatment of ischemic stroke. Cerebrovascular Diseases. 2011;32(4):307-20.

Hermann DM, Mies G, Hossmann KA. Biochemical changes and gene expression following traumatic brain injury: role of spreading depression. Restorative neurology and neuroscience. 1999 Jan 1;14(2-3):103-8.

Horiguchi T, Snipes JA, Kis B, Shimizu K, Busija DW. Cyclooxygenase-2 mediates the development of cortical spreading depression-induced tolerance to transient focal cerebral ischemia in rats. Neuroscience. 2006 Jan 1;140(2):723-30.

Hossmann KA. Periinfarct depolarizations. Cerebrovascular and brain metabolism reviews. 1996;8(3):195-208.

Huntley GW. Synaptic circuit remodelling by matrix metalloproteinases in health and disease. Nature Reviews Neuroscience. 2012 Nov;13(11):743-57.

Imamura K, Takeshima T, Fusayasu E, Nakashima K. MMIncreased plasma matrix metalloproteinase-9 levels in migraineurs. Headache: The Journal of Head and Face Pain. 2008 Jan;48(1):135-9.

Itatsu K, Sasaki M, Yamaguchi J, Ohira S, Ishikawa A, Ikeda H, Sato Y, Harada K, Zen Y, Sato H, Ohta T. Cyclooxygenase-2 is involved in the up-regulation of matrix metalloproteinase-9 in cholangiocarcinoma induced by tumor necrosis factor-α. The American journal of pathology. 2009 Mar 1;174(3):829-41.

Itoh, Y. (2015). Membrane-type matrix metalloproteinases : Their functions and regulations. Matrix Biology. 2015 44–46, 207–223. https://doi.org/10.1016/j.matbio.2015.03.004.

Jabłonka JA. Post stroke plasticity impairment and its depend-ence on interhemispheric interactions. InMEA Meeting 2012 (p. 136).

Jabłonka JA, Burnat K, Witte OW, Kossut M. Remapping of the somatosensory cortex after a photothrombotic stroke: dynamics of the compensatory reorganization. Neuroscience. 2009 Dec.;165(1):90-100.

Jabłonka JA, Kossut M, Witte OW, Liguz-Lecznar M. Experience-dependent brain plasticity after stroke: effect of ibuprofen and poststroke delay. European Journal of Neuroscience. 2012 Sep;36(5):2632-9.

Jabłonka JA, Urbach P, Kazmierczak M, Borzymowska E, Kublik E. Interhemispheric interac-tions contribution in experience dependent plasticity. Neuroscience Meeting Planner. Washington, DC: Society for Neuroscience. 2014. Program No. 246.12/GG26

Jabłonka JA, Witte OW, Kossut M. Photothrombotic infarct impairs experience-dependent plasticity in neighboring cortex. Neuroreport. 2007 Jan 22;18(2):165-9.

Jander S, Schroeter M, Peters O, Witte OW, Stoll G. Cortical spreading depression induces proinflammatory cytokine gene expression in the rat brain. Journal of Cerebral Blood Flow & Metabolism. 2001 Mar;21(3):218-25.

Kaliszewska A, Bijata M, Kaczmarek L, Kossut M. Experience-dependent plasticity of the barrel cortex in mice observed with 2-DG brain mapping and c-Fos: effects of MMP-9 KO. Cerebral Cortex. 2012 Oct 20;22(9):2160-70.

Katagiri T, Hatano N, Aihara M, Kawano H, Okamoto M, Liu Y, Izumi T, Maekawa T, Nakamura S, Ishihara T, Shirai M. Proteomic analysis of proteins expressing in regions of rat brain by a combination of SDS-PAGE with nano-liquid chromatography-quadrupole-time of flight tandem mass spectrometry. Proteome science. 2010 Dec;8(1):41.

Kaufmann D, Theriot JJ, Zyuzin J, Service CA, Chang JC, Tang YT, Bogdanov VB, Multon S, Schoenen J, Ju YS, Brennan KC. Heterogeneous incidence and propagation of spreading depolarizations. Journal of Cerebral Blood Flow & Metabolism. 2017 May;37(5):1748-62.

Kirkby NS, Chan MV, Zaiss AK, Garcia-Vaz E, Jiao J, Berglund LM, Verdu EF, Ahmetaj-Shala B, Wallace JL, Herschman HR, Gomez MF. Systematic study of constitutive cyclooxygenase-2 expression: role of NF-κB and NFAT transcriptional pathways. Proceedings of the National Academy of Sciences. 2016 Jan 12;113(2):434-9.

Koistinaho J, Chan PH. Spreading depression-induced cyclooxygenase-2 expression in the cortex. Neurochemical research. 2000 May 1;25(5):645-51.

Koistinaho J, Pasonen S, Yrjanheikki J, Chan PH. Spreading depression-induced gene expression is regulated by plasma glucose. Stroke. 1999 Jan 1;30(1):114-9.

Kriz J, Lalancette-Hébert M. Inflammation, plasticity and real-time imaging after cerebral ischemia. Acta neuropathologica. 2009 May 1;117(5):497-509.

Küry P, Schroeter M, Jander S. Transcriptional response to circumscribed cortical brain ischemia: spatiotemporal patterns in ischemic vs. remote non-ischemic cortex. European Journal of Neuroscience. 2004 Apr;19(7):1708-20.

Lauritzen M, Strong AJ. 'Spreading depression of Leão'and its emerging relevance to acute brain injury in humans. Journal of Cerebral Blood Flow & Metabolism. 2017 May;37(5):1553-70.

Lee SR, Kim HY, Hong JS, Baek WK, Park JW. PPARγ agonist pioglitazone reduces matrix metalloproteinase-9 activity and neuronal damage after focal cerebral ischemia. Biochemical and biophysical research communications. 2009 Feb 27;380(1):17-21.

Li P, Rudolph U, Huntsman MM. Long-term sensory deprivation selectively rearranges functional inhibitory circuits in mouse barrel cortex. Proceedings of the National Academy of Sciences. 2009 Jul 21;106(29):12156-61.

Li S, Overman JJ, Katsman D, Kozlov SV, Donnelly CJ, Twiss JL, Giger RJ, Coppola G, Geschwind DH, Carmichael ST. An age-related sprouting transcriptome provides

molecular control of axonal sprouting after stroke. Nature neuroscience. 2010 Dec;13(12):1496.

Marik SA, Yamahachi H, McManus JN, Szabo G, Gilbert CD. Axonal dynamics of excitatory and inhibitory neurons in somatosensory cortex. PLoS biology. 2010 Jun 15;8(6):e1000395.

Meighan SE, Meighan PC, Choudhury P, Davis CJ, Olson ML, Zornes PA, Wright JW, Harding JW. Effects of extracellular matrix-degrading proteases matrix metalloproteinases 3 and 9 on spatial learning and synaptic plasticity. Journal of neurochemistry. 2006 Mar;96(5):1227-41.

Michaluk P, Wawrzyniak M, Alot P, Szczot M, Wyrembek P, Mercik K, Medvedev N, Wilczek E, De Roo M, Zuschratter W, Muller D. Influence of matrix metalloproteinase MMP-9 on dendritic spine morphology. J Cell Sci. 2011 Oct 1;124(19):3369-80.

Michelson NJ, Kozai TD. Isoflurane and ketamine differentially influence spontaneous and evoked laminar electrophysiology in mouse V1. Journal of neurophysiology. 2018 Aug 1;120(5):2232-45.

Miettinen S, Fusco FR, Yrjänheikki J, Keinänen R, Hirvonen T, Roivainen R, Närhi M, Hökfelt T, Koistinaho J. Spreading depression and focal brain ischemia induce cyclooxygenase-2 in cortical neurons through N-methyl-D-aspartic acid-receptors and phospholipase A2. Proceedings of the National Academy of Sciences. 1997 Jun 10;94(12):6500-5.

Mohajerani MH, Aminoltejari K, Murphy TH. Targeted mini-strokes produce changes in interhemispheric sensory signal processing that are indicative of disinhibition within minutes. Proceedings of the National Academy of Sciences. 2011 May 31;108(22):E183-91.

Monea S, Jordan BA, Srivastava S, DeSouza S and Ziff EB. Membrane Localization of Membrane Type 5 Matrix Metalloproteinase by AMPA Receptor Binding Protein and Cleavage of Cadherins. Journal of Neuroscience. 2006 Feb 22; 26 (8) 2300-2312.

Nagel S, Sandy JD, Meyding-Lamade U, Schwark **C,** Bartsch JW, Wagner S. Focal cerebral ischemia induces changes in both MMP-13 and aggrecan around individual neurons. Brain research. 2005 Sep 14;1056(1):43-50.

Nedergaard M, Hansen AJ. Spreading depression is not associated with neuronal injury in the normal brain. Brain research. 1988 May 24;449(1-2):395-8.

Neumann-Haefelin T, Witte OW. Periinfarct and remote excitability changes after transient middle cerebral artery occlusion. Journal of Cerebral Blood Flow & Metabolism. 2000 Jan;20(1):45-52.

Nonose Y, Gewehr PE, Almeida RF, da Silva JS, Bellaver B, Martins LA, Zimmer ER, Greggio S, Venturin GT, Da Costa JC, Quincozes-Santos A. Cortical bilateral adaptations

in rats submitted to focal cerebral ischemia: emphasis on glial metabolism. Molecular neurobiology. 2018 Mar 1;55(3):2025-41.

Ou Z, Zhao X, Labiche LA, Strong R, Grotta JC, Herrmann O, Aronowski J. Neuronal expression of peroxisome proliferator-activated receptor-gamma (PPARγ) and 15d-prostaglandin J2—Mediated protection of brain after experimental cerebral ischemia in rat. Brain research. 2006 Jun 22;1096(1):196-203.

Overman JJ, Clarkson AN, Wanner IB, Overman WT, Eckstein I, Maguire JL, Dinov ID, Toga AW, Carmichael ST. A role for ephrin-A5 in axonal sprouting, recovery, and activity-dependent plasticity after stroke. Proceedings of the National Academy of Sciences. 2012 Aug 14;109(33):E2230-9.

Que M, Schiene K, Witte OW, Zilles K. Widespread up-regulation of N-methyl-D-aspartate receptors after focal photothrombotic lesion in rat brain. Neurosci Lett. 1999 Oct 1;273(2):77-80.

Phillips LL, Chan JL, Doperalski AE, Reeves TM. Time dependent integration of matrix metalloproteinases and their targeted substrates directs axonal sprouting and synaptogenesis following central nervous system injury. Neural regeneration research. 2014 Feb 15;9(4):362.

Piilgaard H, Lauritzen M. Persistent increase in oxygen consumption and impaired neurovascular coupling after spreading depression in rat neocortex. Journal of Cerebral Blood Flow & Metabolism. 2009 Sep;29(9):1517-27.

Potworowski J, Jakuczun W, Łęski S, Wójcik DK. Kernel current source density method. BMC neuroscience. 2011 Dec;12(1):P375.

Redecker **C,** Wang W, Fritschy JM, Witte OW. Widespread and long-lasting alterations in GABAA-receptor subtypes after focal cortical infarcts in rats: mediation by NMDA-dependent processes. Journal of Cerebral Blood Flow & Metabolism. 2002 Dec;22(12):1463-75.

Reinhard SM, Razak K, Ethell IM. A delicate balance: role of MMP-9 in brain development and pathophysiology of neurodevelopmental disorders. Frontiers in cellular neuroscience. 2015 Jul 29;9:280.

Romanic AM, White RF, Arleth AJ, Ohlstein EH, Barone FC. Matrix metalloproteinase expression increases after cerebral focal ischemia in rats. Stroke. 1998 May 1;29(1020):30.

Samad TA, Moore KA, Sapirstein A, Billet S, Allchorne A, Poole S, Bonventre JV, Woolf CJ. Interleukin-1β-mediated induction of Cox-2 in the CNS contributes to inflammatory pain hypersensitivity. Nature. 2001 Mar;410(6827):471.

Sang N, Chen C. Lipid signaling and synaptic plasticity. The Neuroscientist. 2006 Oct;12(5):425-34.

Schiene K, Bruehl **C,** Zilles K, Qu M, Hagemann G, Kraemer M, Witte OW. Neuronal hyperexcitability and reduction of GABAA-receptor expression in the surround of cerebral photothrombosis. Journal of Cerebral Blood Flow & Metabolism. 1996 Sep;16(5):906-14.

Shinohara M, Dollinger B, Brown G, Rapoport S, Sokoloff L. Cerebral glucose utilization: local changes during and after recovery from spreading cortical depression. Science. 1979 Jan 12;203(4376):188-90.

Sommer CJ. Ischemic stroke: experimental models and reality. Acta neuropathologica. 2017 Feb 1;133(2):245-61.

Strominger RN, Woolsey TA. Templates for locating the whisker area in fresh flattened mouse and rat cortex. Journal of neuroscience methods. 1987 Dec 1;22(2):113-8.

Tailby **C,** Wright LL, Metha AB, Calford MB. Activity-dependent maintenance and growth of dendrites in adult cortex. Proceedings of the National Academy of Sciences. 2005 Mar 22;102(12):4631-6.

Theriot JJ, Toga AW, Prakash N, Ju YS, Brennan KC. Cortical sensory plasticity in a model of migraine with aura. Journal of Neuroscience. 2012 Oct 31;32(44):15252-61.

Thompson CS, Hakim AM. Cortical spreading depression modifies components of the inflammatory cascade. Molecular neurobiology. 2005 Aug 1;32(1):51-7.

Urbach A, Bruehl **C,** Witte OW. Microarray-based long-term detection of genes differentially expressed after cortical spreading depression. European Journal of Neuroscience. 2006 Aug;24(3):841-56.

Victor NA, Wanderi EW, Gamboa J, Zhao X, Aronowski J, Deininger K, Lust WD, Landreth GE, Sundararajan S. Altered PPARγ expression and activation after transient focal ischemia in rats. European Journal of Neuroscience. 2006 Sep;24(6):1653-63.

Wang X, Jung J, Asahi M, Chwang W, Russo L, Moskowitz MA, Dixon CE, Fini ME, Lo EH. Effects of matrix metalloproteinase-9 gene knock-out on morphological and motor outcomes after traumatic brain injury. Journal of Neuroscience. 2000 Sep 15;20(18):7037-42.

Wang XB, Bozdagi O, Nikitczuk JS, Zhai ZW, Zhou Q, Huntley GW. Extracellular proteolysis by matrix metalloproteinase-9 drives dendritic spine enlargement and long-term potentiation coordinately. Proceedings of the National Academy of Sciences. 2008 Dec 9;105(49):19520-5.

Witte OW, Bidmon HJ, Schiene K, Redecker **C,** Hagemann G. Functional differentiation of multiple perilesional zones after focal cerebral ischemia. Journal of Cerebral Blood Flow & Metabolism. 2000 Aug;20(8):1149-65.

Woessner Jr JF. Matrix metalloproteinases and their inhibitors in connective tissue remodeling. The FASEB Journal. 1991 May;5(8):2145-54.

Xue J, Hua YN, Xie ML, Gu ZL. Aspirin inhibits MMP-9 mRNA expression and release via the PPARα/γ and COX-2/mPGES-1-mediated pathways in macrophages derived from THP-1 cells. Biomedicine & Pharmacotherapy. 2010 Feb 1;64(2):118-23.

Yin KJ, Deng Z, Hamblin M, Zhang J, Chen YE. Vascular PPARδ protects against stroke-induced brain injury. Arteriosclerosis, thrombosis, and vascular biology. 2011 Mar;31(3):574-81.

## STAR Methods

**We compared** (Tab.1)**:**

(**I**) the whiskers cortical representations and

(**II**) the general metabolic activity pattern

between groups of the:

**a)** intact animals (n=6),

**b)** the animals after ExDP induction by cutting all except row B whiskers for one month (**C**, n=6)

and this results with ExDP efficacy observed after:

**c)** SDs induced by hyperosmolar KCl dura application (**SD**, n=8),

**d)** hyperosmolar NaCl instead of KCl application in sham animals (**SDS**, n=5),

**e)** PiDs induced by focal cortical stroke (**Pt**, n=6).

That led us to comparison of

(**III**) Electrophysiological (n=6 for each group) and

(**IV**) Proteomic differences (n > 5 in each group) between all the groups.

(The numbers from **I** to **IV** will be used as a reference to the specific experimental schemes related to these goals throughout the text).

### Animals

The experimental protocols were in accordance with the European Communities Council Directive (86/609/EEC) and approved by the local authority (Thueringer Landesamt, Bad Langensalza, Germany (02-20/05) and 1st Ethical Commission in Warsaw, Poland (270/2012, 660/2016).

Male Wistar rats weighing 290±20g (about 3 months old) were used for the experiments. Animals were kept in constant 12 hour light/dark conditions with food and water access ad libitum. Rats were randomly assigned to 13 experimental groups. (**I, II**) Three of the groups were for testing the dynamics of experience-dependent plasticity after SD: with SD-induced (**SD**), sham (**SDS**) and control (**SDC**) with the SD-like surgery and whiskers deprivation after that. The additional group with the PtS induction were to confirm our previous description of post-stroke metaplasticity changes (**Pt**). All were referred to as intact controls and controls with ExDP induced (**C**). SD-operated groups and additional with stroke induction had single channel recordings for depolarizations confirmation and comparison to spontaneous activity during the operation conditions (**IIIA**). (**IV**) Four other groups were included for proteins studies by Western Blot. In all the experimental groups with procedure IV electrophysiological brain

activity was measured with multielectrode recordings (**IIIB**). For monitoring PiDs after PtS we included an additional group of rats with electrophysiological recordings during PtS.

***Surgeries***

During all operating procedures the animal's heart and breathing rates were monitored continuously. The blood saturation with body temperature was also controlled (SOx 98% 1%; 36.5° **C**±0.5°C; MouseOx Plus, Starr). To prevent dehydration and maintain an adequate level of nutrition every second hour of narcosis, if required, animals were given additional subcutaneous injections of 2 ml saline or Duphalyte (solution of amino acids, mineral ions, and carbohydrates; Pfizer OLOT, Spain).

**SD-like surgery (Ib,Ic,II, IIIa, IIIb, IV)**

30 animals had SD-like surgeries. (I, II) For the ExDP studies animals (n=18) were anesthetized with 2.5% isoflurane in $N_2O/O_2$ (60/30 l/h) and fixed in a stereotactic frame. The skull was exposed by an incision along the midline and two trepanations were drilled over the right hemisphere, (1.8 mm in diameter; coordinates: bregma -6.8 and bregma +2, both 2 mm from midline) leaving the dura intact. After reduction of anesthesia to 1.5% isoflurane, solutions were applied to the brain at the posterior trepanation (sol) for about 2 hours: 3M KCl (**SD** group), 3M NaCl (sham – **SDS**) or aCSF (control – **SDC**). Finally, trepanations and wounds were closed. To verify the occurrence of **SD** we concurrently recorded the electrocorticogram and direct current potential at the anterior position with a single electrode. Therefore, we placed a glass electrode (2 to 4MΩ) filled with aCSF (120 NaCl, 2 CaCl2, 5 KCl, 1.8 MgCl2, 10 HEPES, 1.25 NaH2PO4 and 10 Glucose: in mmol/L) and containing an Ag/AgCl wire on the dura exposed in the anterior craniotomy. An Ag/AgCl-reference electrode was placed subcutaneously in the neck.

(III, IV) During the operations intended for further studies of protein expression changes and for setting a more precise electrophysiological recordings the frontal trepanation was made a bit wider and a row of 16 electrodes (1.6 mm wide) were positioned on the dura to visualize direct spread of **SD** waves (coordinates: bregma +1—+4, 2,5 mm wide, for electrode positioning 5 mm from the midline, n=17) (Fig. 1A).

**Photothrombotic stroke surgery (Id, II, IIIa, IV,V)**

Photothrombotic stroke was conducted in the right hemisphere cortex of 17 animals. Animals were anesthetized and the skull was exposed as was described for SD-operated groups. Rose Bengal (0.4 ml, 10 mg/ml; 330000; Sigma-Aldrich, St Louis, MO, USA) was injected. After drilling the trepanation for electrophysiological recording the fibre-optic bundle light center (aperture=1.5 mm) was placed on the cleaned skull bone.

● (I, II, IIIa) over the back frontal trunk sensory representation (***s***, coordinates: bregma - 4.5 mm and 4 mm lateral from the midline (Fig. 1A)) in a vicinity of the somatosensory cortical representation of whiskers which plasticity was induced: (I,II) to confirm our previously published results showing that unilateral PtS impairs ExDP and compare it to SD-operated groups and (IV) for the analysis of the proteins expression changes to compare the conditions for the ExDP after stroke with the conditions of SD-operated groups;

● (IIIa) over the visual area of the occipital cortex to facilitate direct comparison of **SD** electrophysiological features to the PiDs occurring during ischemia (coordinates: bregma -5, 3 mm lateral (Fig.1A)) with corticogram measured from the dura above the prefrontal cortex by a single glass electrode (like during the described above SD-like surgery I, II; coordinates: bregma +2mm, 2 mm lateral to the right; with trepanation 1.8 mm in diameter).

***Electrophysiological recordings*** *(IIIa,IIIb)*

The electrocorticograms (ECoGs) were recorded over a period of about 2h starting at least 2 minutes before the application of salt solutions in SD-operated rats or before Bengal Rose injection in **Pt** group.

The recording electrodes were placed on the dura surface as described in operation sections. All data were transferred to a PC computer for online display analysis, and data storage using a high impedance amplifier (EXT-08, NPI, Tamm, Germany (for glass electrodes) or for the tungsten electrodes the A-M Systems amplifier, model: 3600 with preamplifier attached directly to the socket of the electrodes holder). Signals from all electrodes were band-pass filtered (0.3 – 5000 Hz) and transformed by CED 1401 Plus analog/digital converter. Software Spike2 (Cambridge Electronic Design, UK) were used for signals digitalization at 19 kHz sampling rate per channel.

Whisker deprivation and $^{14}$C-2-DG brain mapping

***Deprivation and brain tissue preparation*** *(I)*

Immediately after the surgery, all left-side whiskers (contralateral to the SD) except that of row B were trimmed close to the skin, and trimming was repeated every second day. After four weeks of deprivation, we performed $^{14}$C-2-deoxy-D-glucose (American Radiolabeled Chemicals; St.Louis, MO, USA) brain mapping. Rats were immobilized and whiskers were cut bilaterally except rows B. The 2-DG was injected intramuscularly (10 μCi/100g body mass) and the rows B of whiskers on both sides of the snout were stimulated simultaneously at a frequency of 2 Hz. After 30 minutes of stimulation, animals were deeply anesthetized by intraperitoneal injection of 1 ml Vetbutal and intracardially perfused with 4%

paraformaldehyde (Sigma-Adrich; St.Louis, MO, USA). The brains were removed and cortices of separated hemispheres were flattened between glass slides to 3 mm, snap frozen in heptane at -70°C and stored at -80°C.

***2-DG incorporation imaging*** *(I, II)*

Flattened hemispheres were cut tangentially on a cryostat at -16°**C** into 40 µm sections, which were collected alternately on slides and coverslips. The sections on coverslips were immediately dried and exposed on Kodak Mammography film for 2 weeks together with a set of [$^{14}$C] standards (ARC 146; American Radiolabeled Chemicals; St.Louis, MO, USA;) and later stained in Nissl staining visualizing neuronal polyribosomes. The remaining sections were stained for mitochondrial cytochrome oxidase activity to identify the barrel field and the lesion regions.

Protein extraction and Western blot (IV)

***Tissue samples***

The levels of chosen proteins (COX-2, MMP-9, MMP-3, MMP-2) were analyzed using Western blot analysis for homogenates of chosen areas isolated 24 h after SDs episodes or stroke induction. Tubulin, GAPDH and total protein with Coomassie Blue were used as a loading control. Tissue samples were collected from rats killed by decapitation. Brains were dissected on ice and tissue samples were immediately transferred to proteinases inhibitors (10% PiC solution), frozen in the liquid nitrogen and stored at -70°C.

The cortical samples were isolated by an absorption (with 2 mm in diameter tube) of the column from the cortical surface to white matter (white matter excluding). The tissue samples were taken bilaterally from the barrel fields (Strominger and Woolsey, 1987), stroke area (s) and area of solutions application (sol) and additionally from the auditory, prefrontal cortex and thalamus (Katagiri et al., 2010). The blots with all groups for each area were done.

***Proteins isolation***

After the addition of an ice-cold RIPA buffer (50 mM Tris, pH 7.5, 150 mM NaCl, 1% NP40, 0.5% sodium deoxycholate, 0.1% sodium dodecyl sulfate, 1 mM ethylenediaminetetraacetic acid, 1 mM NaF, Complete Protease Cocktail and Phosphatase Inhibitor Cocktail 2) the tissue samples were homogenized by sonication, centrifuged, and stored at -80°C.

***Western blots***

Since we were looking for differences potentially influencing cortical plasticity, the blots were designed for homogenates from the precise area from each group together.

Proteins were separated in sodium dodecyl sulfate-acrylamide gels and transferred to PVDF membrane. PageRuler™. Prestained Protein Ladder was used as a size standard (26616, Thermo Fisher Scientific). The membranes were blocked with non-fat dry milk and incubated overnight with primary antibodies at 4°**C** (Abcam polyclonal rabbit IgG: Anti-MMP2 – ab37150, Anti-MMP3 – ab53015, Anti-MMP9 – ab38898, Anti-COX-2 – ab15191 and Abcam mouse monoclonal anti-beta III Tubulin IgG2a – ab78078, anti-GAPDH, SantaCruz, SC-25772). After washing, the membranes were incubated with peroxidase-coupled secondary IgG antibodies (anti-Rabbit– A0545 or anti-Mouse –A9044, Sigma Aldrich) for 2 h at room temperature. Staining was then visualized by chemiluminescence. The images were captured using an ImageQuant LAS 4000.

Data analysis and statistics (Dast)

Assuming the dynamics of the cortical experience-dependent plasticity, in response to deprivation, depends on the global CNS changes presented exclusively after stroke and differentiating this group from the rest, we concentrated on the metabolic activity changes (2-DG), proteomic (Wb) and electrophysiological properties specific to the post-stroke group. Since we were not able to control all factors the results which exceeded twice the standard deviation were excluded or described separately. When results of one or two rats enhanced the **SD** over the mean value they were also mentioned separately. Values of $p < 0.05$ were considered statistically significant and standard deviation (SD) shown as within-group data differences.

***DaSt: 2-DG incorporation, histological stainings and Western blots***

The autoradiograms, blots and histological images were analyzed by a computer image analysis program (MCID, M4 Res Inc., Ontario, Canada). The program enables to measure precisely the optical density (OD) in 8-16 or 24 bit accuracy. The OD and distance were calibrated. Blots densitometric analyses were also performed using Quantity One 1-D software (Bio-Rad) and compared with that made by MCID.

The differences between groups were tested using a multi-factor ANOVA and a post-hoc Tuckey test (for unequal N). The significance of the differences between the hemispheres was calculated with a two-tailed paired Student's T-test.

***DaSt: Histological tissue analysis*** *(I, II, IIIa)*

The color images of histologically stained sections were coded in 24 bits. The software allowed us to display on screen the image of a Nissl stained section from which the autoradiogram was obtained and adjacent sections stained for cytochrome oxidase activity and

superimpose these pictures on each other so that the relation of the barrel field to the position of the electrodes, lesions or solution application areas could be precisely measured.

The tangential sections of KCl and NaCl treated groups do not permit for a closer study of the lesion size and distribution. Therefore, we measured the lesion diameter on the surface of the brain (the widest place) and its shortest distance to the barrel cortex on the surface of the unprepared flattened hemisphere and on slices from layer IV, where the barrel field was visible. The diameter of the stroke was also measured on the layer IV tangential sections. Lesions depth was measured basing on the extrapolated edge of the tangential slice in the place of the tissue destroyed by the lesion and its distance to the deepest place of lesion bottom (Fig. 1A).

**DaSt: 2-DG incorporation** (I, II)

The 2-DG incorporation level was measured on standardized images of the sections autoradiograms. The grayscale images of autoradiograms were analyzed in 8 bits accuracy with 255 gray scale levels.

**DaSt: Experience dependent plasticity** (I)

The width of the labeled cortical representation of row B whiskers was measured in layer IV. The pixels with 2-DG-uptake intensity continuously above 15% of the mean surrounding cortex incorporation were considered as the labeled representation. The results were averaged for all sections from layer IV of one hemisphere.

**DaSt: Metabolic correlates of cortical activity** (II)

To determine the metabolic rate in different cortical regions we applied a semi-quantitative method based on the densitometry measures from [$^{14}$C] 2DG autoradiograph. Assuming that the OD in autoradiographs is proportional to the concentration of the [$^{14}$C] isotope that in turn reflects local glucose consumption (Sokoloff et al. 1977), we converted the OD values from digitized images into μCi based on the ODs of the[$^{14}$C] standards that were co-exposed with the cortex sections. [$^{14}$C] 2DG uptake was measured on tangential sections and averaged for cortical layers II/III, IV and V/VI. Regions of interest were defined on Nissl stains of the sections that produced the autoradiograph and neighboring this stained for cytochrome oxidase activity.

(I) For evaluating metabolic activity in the representation of the spared row B whiskers, we considered their primary somatosensory representation (BF), their secondary somatosensory representation (SII) and the auditory cortex (Au) as a control. (II) For measuring the effects of **SD** or stroke on cortical metabolic activity, we analyzed OD from the entire cortex but omitting the highly activated row B and auditory cortical primary representations. For each region also

the ratio of the homotopic areas in intact to treated, deprived hemisphere was compared between groups.

***DaSt: Western blots*** *(IV)*

Since we used 8 bits grayscale images the 255 gray scale levels were satisfying. The MCID programme can perform the line analysis designed for electrophoresis with "pick detection" and "smiling correction" (Fig. 1D).

After background subtraction, the protein of interest was normalized to housekeepers and multiplied by the surface of the analyzed protein strip (mostly ß-tubulin but for s tissue samples also GABDEH was used due to evident inter-group differences in tubulin concentration). The normalized abstract number of the protein amount [An] was used for data presentation. The OD exceeding the background over 10 % (5 An) (Fig. 1D & Supp. Fig. 2) were treated as a proof of protein present in homogenate. The final An for each animal were compared between groups present on one blot, but also some inter-bolts comparisons were described.

The correlations for proteins relations between groups in different areas and between particular animals in each group were performed and compared for each blot. When a band of one or two rats enhanced the **SD** above the mean value they were mentioned separately (as "+ xx [An]").

**DaSt: Additional group specific bands**

Due to some changes differentiating the experimental groups observed in additional bands of lower or higher molecular weight (Supp. Fig 3), they were also considered as valuable information and had OD measured (Supp. Fig. 5) which is presented in supplementary data. Heavier (protein+X) and lighter (protein-X) bands were considered separately. For comparing groups with unequal variances (usually in the additional bands on blots) Mann-Whitney (MW) test was performed compensated by Bonferroni correction for testing six hypotheses. Thus, the established statistically significant p-value was p=0.008.

***DaSt: Electrophysiological brain activity*** *(III)*

Analyses of the electrophysiological data were made using Python programing language and Matlab (MathWorks) statistical tools.

**DaSt: Electrophysiological data pre-processing**

**DaSt: Single electrode recordings** (IIIa)

To visualize basic electrical activity during spreading depolarization we recorded raw signal from one glass electrode at the dura level. To establish depolarization time we applied a "moving variation" method for low pass <0.1 Hz filtered signal. Depolarization for

comparisons was averaged across depolarization trials in PiDs (n=16) and SDs (n=10) (Fig1A) and then compared between groups (Fig 1B).

We filtered signal 0.1-100 Hz with a third order Butterworth filter to show a significant decrease in spontaneous activity during spreading depression. We computed spectrograms, for 50 minutes band-pass filter signal. In order to search for electrophysiological differences between PiDs and SDs, we have chosen fragments ±250 seconds from continuous signal around the trough of the significant depolarization sites and we treated them as trials for further analysis. Next, we filtered signal 0.1-50 Hz and calculated spectrograms using 5-sec non-overlapping window.

**DaSt: Multielectrode recordings** (IIIb)

To watch closely the spreading of the slow depolarization waves the SDs signal was recorded later with 14 channel tungsten electrode with 19.6 kHz frequency. We filtered the signal with a 4th order filter, low-pass from 1 Hz. The sampling rate was reduced from the original sampling rate by a factor of two, from the 19608 Hz to 9804 Hz.

**DaSt: Electrophysiological statistics** (IIIa, IIIb)

Most differences between frequency bands were tested using a multi-factor ANOVA and a post-hoc Wilcoxon test. To estimate significant differences between groups we used also the resampling method. We picked (10 000 times) random depolarization fragments and calculated mean spectrogram for this new random sets. As a statistic, we used the difference in every "pixel" calculated for groups and compared it with the original difference between PiDs and SDs. As a result, we got the p-value for every "pixel" for average spectrogram picture (Supp. Fig. 1).

**CSD analysis**

To estimate the distribution of current source and sinks of the depolarization event recorded at multiple sites we used kCSD reconstruction method (Potworowski et al., 2012). We assumed constant and isotropic tissue conductivity for CSD reconstruction.

**Nomenclature**

For easier accommodation of the huge amount of data and easier document navigation, we use a few different formatting rules and some abbreviations for different types of data. Brain regions examined in the experiment will be an abbreviation written in italic bold (***BF, sol, s, Th***). Experimental groups will be in bold uppercase (**C, SDC, SD, SDS, S**).

**Abbreviations**

2-DG – $^{14}$C-2-deoxyglucose; Au – auditory cortex; BF – barrel field; ECoG – electrocorticograms; ExDP – experience-dependent plasticity; Hp –hind paw; *MW* – Mann-Whitney test OD – optical density; OS – open source; PiD – peryinfarct depolarization; PtS – photothrombotic stroke; ***s*** – stroke area with the PtS induced in the **Pt** group; SII – secondary somatosensory cortex; ***sol*** – solution application area; **SD** – spreading depolarization in contrast to experimental group **SD** and *SD* – standard deviations; ***th*** – thalamus;

**Availability of data and materials:**

The manuscript data will be stored at Research Gate profile of corresponding author.

**Acknowledgements**

We would like to thank Prof. Marta Wiśniewska for her help in protein studies and Prof. Ewa Kublik for her help in electrophysiology and especially Dr. rer. nat. Anja Urbach and Prof. Otto Witte for their continuous support and sharing their data and to Prof. Małgorzata Kossut for supporting the scientific development.

Jan Jabłonka and collaborators were funded by grants: MNiSW 1008/PO1/2007/22; 0184/IP1/2011/71, 0292/IP1/2013/72.

Paulina Urban was funded by grant number NCN 2014/15/B/ST6/05082.

**Author Contributions**

| Activity Category | | JJ | CM | MS | WS | PU | LS | MW | AS |
|---|---|---|---|---|---|---|---|---|---|
| Conceptualizing a research idea | **90** | 70 | | 10 | 3 | 2 | 3 | 2 | |
| Refining/ crystalizing a research idea | **60** | 30 | | 10 | 5 | | 8 | 5 | 2 |
| Literature search: Summarizing literary pieces (e.g., articles, book chapters, etc.) | **20** | 10 | | 5 | 2 | 1 | | | 2 |
| Creating a research design (e.g., counterbalancing, randomization to conditions, survey design etc.) | **80** | 40 | 2 | 15 | 10 | | 5 | | 8 |
| Selecting an Instrument/ a measure: Instrument construction | **30** | 19 | 1 | 3 | 3 | | 2 | | 2 |
| Selection of statistical tests/analyses<br>Performing statistical analyses and computations | **40** | 20 | 2 | 2 | 8 | 3 | 2 | 3 | |
| (including computer work) | **40** | 10 | 3 | 5 | 9 | 7 | | 6 | |
| Interpretation of statistical analyses | **80** | 35 | 1 | 12 | 15 | 5 | 5 | 5 | 2 |
| **Manuscript** | | | | | | | | | |
| Writing an introduction section | **90** | 70 | | 5 | 4 | 5 | 2 | 2 | 2 |
| Writing a methods section | **80** | 60 | | | 8 | 5 | 5 | 2 | |
| Writing results section | **80** | 45 | | 15 | 8 | 5 | 2 | 3 | 2 |
| Writing discussion section | **100** | 60 | | 20 | 10 | 3 | 3 | 2 | 2 |
| Writing conclusive summary | **60** | 45 | | 5 | 5 | 2 | | | 3 |
| Writing limitations of the study | **60** | 40 | | 10 | 5 | | 5 | | |
| Writing future directions of the study | **60** | 45 | | 5 | 3 | | | 2 | 5 |

**Declaration of Interests**

The authors declare no competing interests.

## Figure Legends

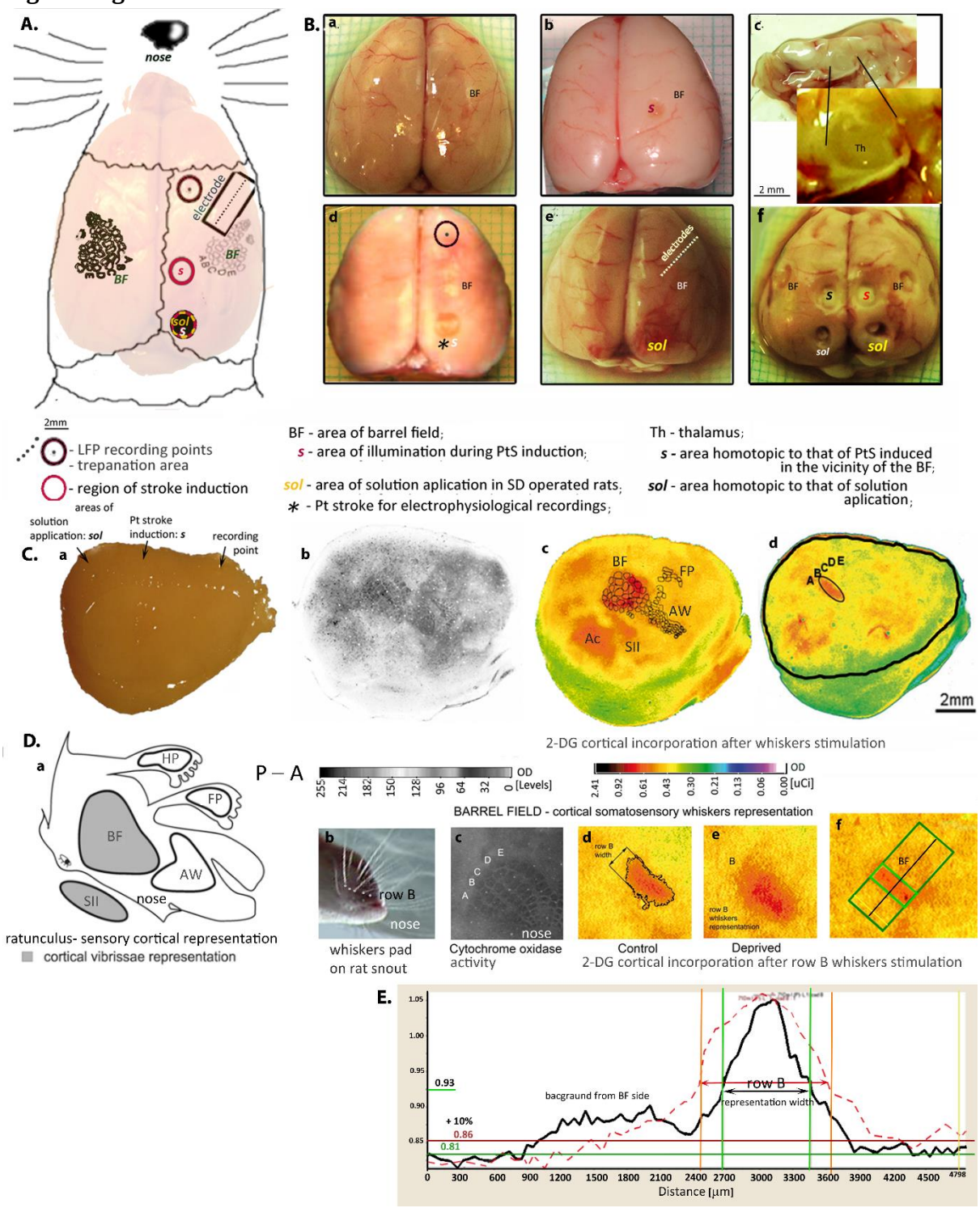

**Fig. 1.**: Examples of experimentally treated brains and further cortical treatment for activity mapping.

**1A:** The schematic drawing shows, relatively to the area of barrel field (BF), foci of the spreading depolarizations accompanying ExDP initiation (region of the photothrombotic stroke induction (***s***), and solution application (***sol***)), location of the electrodes (the ECoG recording points) and the skull trepanation areas.

**1B:** Photos of isolated brains for: 2DG brain mapping of ExDP (1B: a,b,d) electrophysiological recordings of PiDs and SDs (1B: c, d) and samples isolation for protein analysis (1B: a,b,d, e,f); from: Control (1B.a), **Pt** (1B: b,e,f) and SD/**SDS**/**SDC** (1B: e,f) animals. Brain prepared for thalamus (1B.f) and cortical samples (1B.e) isolation from: BF, ***sol*** and ***s***.

**1C:** Flatted hemisphere for tangential sectioning of the cortex for further 2DG brain mapping visualization (1C.a) with a marked position of ***sol***, Pt stroke induction (***s***) and ECoG recording point. Localization of the rats' cortical whiskers somatosensory representations on a tangential section of layer IV (1C: b,c,d): stained by Nissl staining (1C.b) with 2DG-incorporation visualized on autoradiograms (1C: c,d), shown in pseudocolors. (AW) anterior whiskers representation; (FP) front paw representation; (SII) secondary somatosensory cortex. Measurements were also taken in (Ac) auditory cortex

**1D:** A cartoon of cortical vibrissal representation in SI and SII. (1D.a)"Rattunculus" with areas of increased activation during all the whiskers stimulation. The whiskers stimulation in intact rats activates contralateral BF and SII and do not activate AW, hind paw (HP) and FP cortical representations. (1D.b) Photo of the whiskers pad on rat snout showing the row B. (1D.c) Magnification of the barrel field on the cortical tangential section after staining for cytochrome oxidase activity. (1D: d,c) a magnification of the row B cortical representation, on digitized autoradiograms of tangential sections, in control (1D.d) and deprived (1D.e) animals. 1D.f) The row B representation in the barrel field with the marked area of OD measure.

**1E:** Comparison of the OD graphs showing 2DG incorporation in non-deprived (black line) and deprived BF (dashed red line). OD analysis by the MCID program, where the area exceeding the background over 10 % were treated as the activated representation of the rows B. Background treated as a reference where the mean value of OD from the neighborhood of the BF (right side of the graph). OD—optical density in arbitrary units with a direct set of 255 gray scale levels or calibrated to µCi radiation units of $^{14}$C-2DG; P–A—posterior to anterior (Supp. Fig. 5).

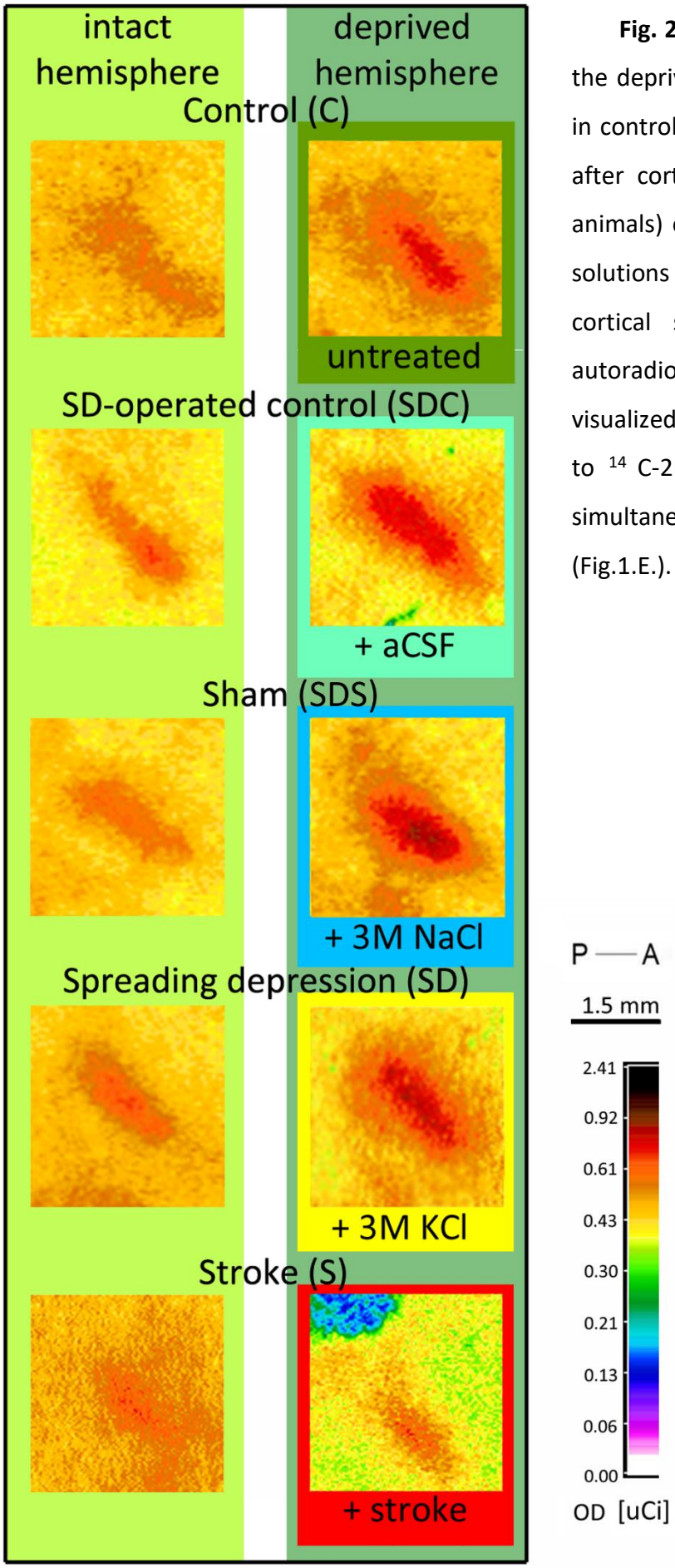


**Fig. 2.:** Rows B cortical representations in the deprived and non-deprived hemispheres: in control animals (C), after PtS (in Pt group); after cortical treatment with: aCSF (to SDC animals) or application of the highly osmotic solutions of NaCl (in SDS) or KCl (in SD) to V2 cortical surface. The magnified parts of autoradiograms of cortical tangential sections, visualized by the exposition of the brain slices to $^{14}$C-2DG incorporations during bilateral, simultaneous rows B whiskers stimulation (Fig.1.E.).

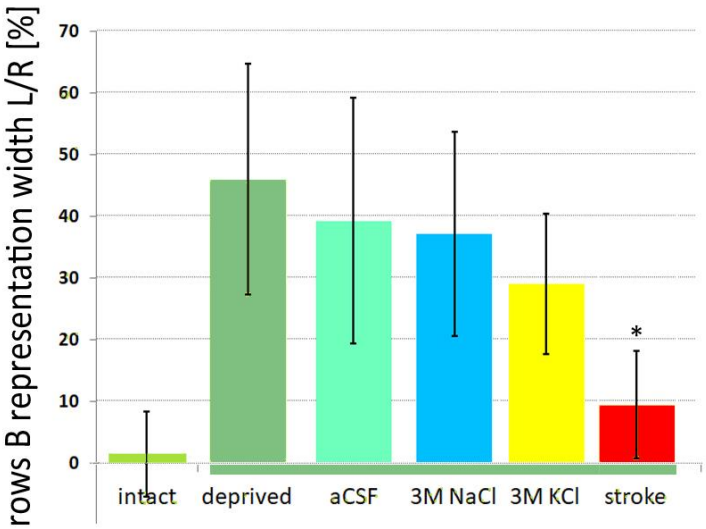


**Fig. 3.**: The ratio in percentage of the rows B representations width in the non-deprived and deprived hemispheres. There was a significant difference in each group except the Pt which did not differ from intact group The Pt-group had significantly lower width in comparison with every other group ($p < 0,001$).

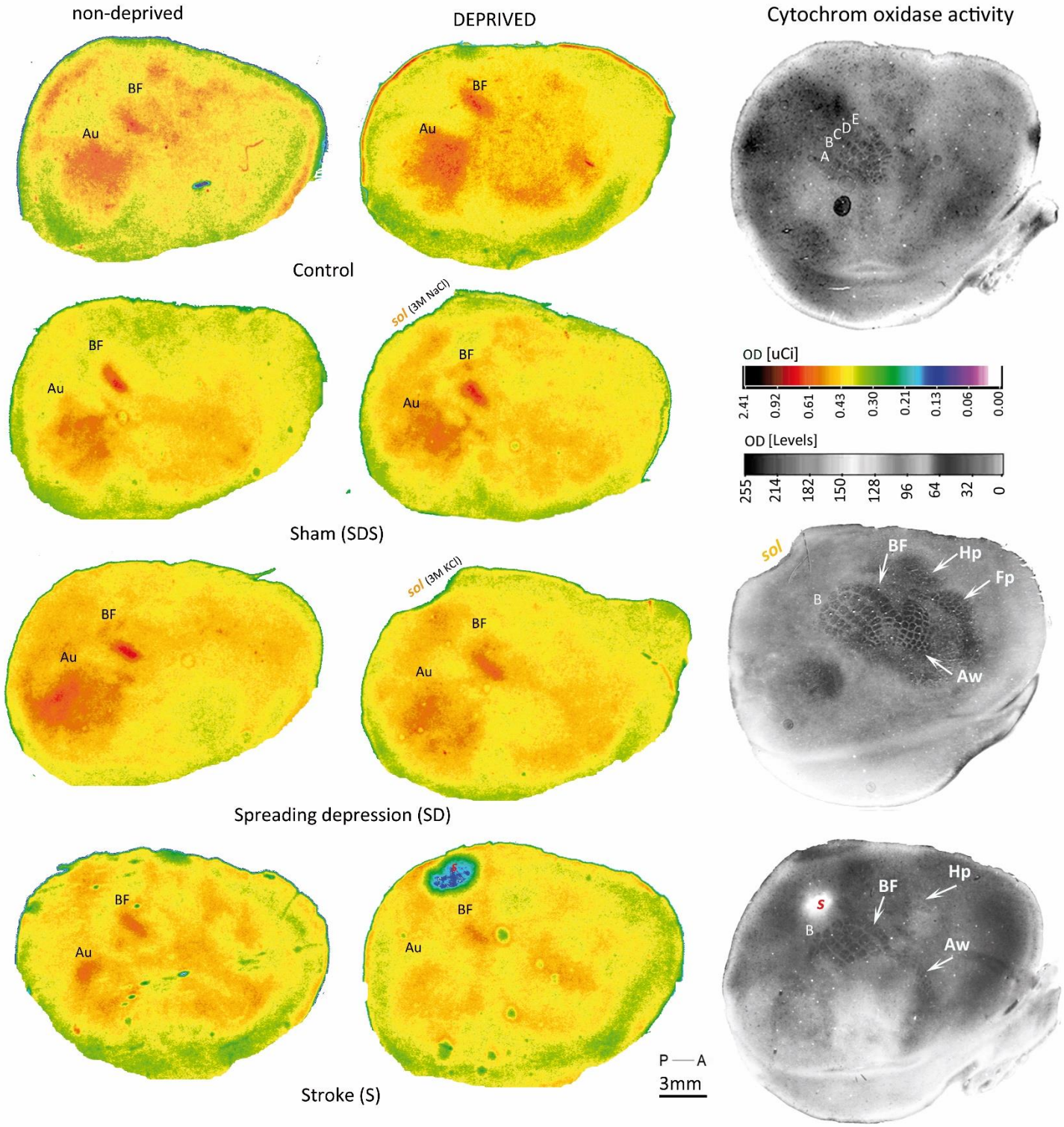


**Fig. 4.** Cortical metabolic activity during the brain mapping with bilateral rows B whiskers stimulation one month after any treatment. 2DG incorporation shown on autoradiograms of entire hemispheres, layer IV, tangential sections. Comparison between the experimental groups (control, stroke, SD-operated: control (**SDC**), sham (**SDS**) and **SD**; for more details see Table 1) with intact (left, A) and deprived (right, B) hemispheres. On the right, the equivalent sections stained for cytochrome oxidase activity (C). A and B showed in pseudocolors (OD—optical density in arbitrary units).

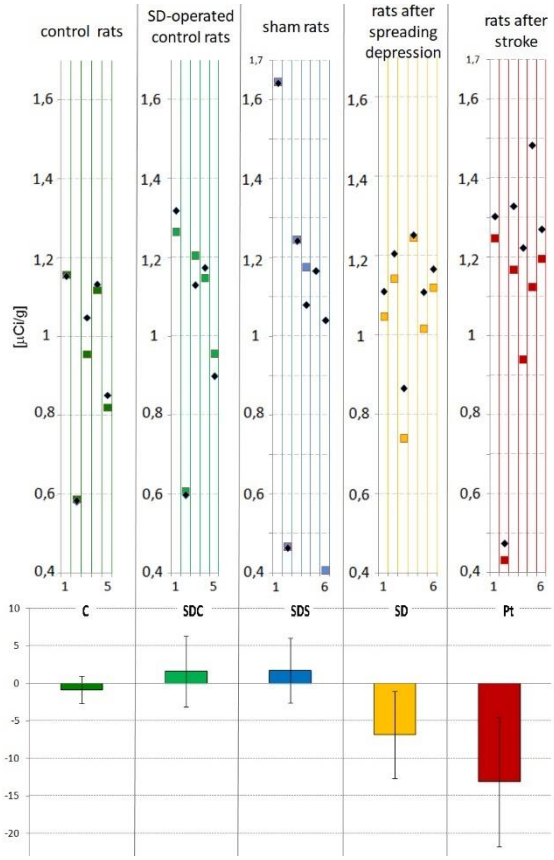


**Fig. 5.** Cortical layer IV 2DG incorporation in the treated and intact hemispheres. Higher graphs represent individual results for each tested animal. Squares represent right hemisphere, diamond – left one. The lower graph shows the interhemispheric comparison of the mean ratio (right to the left hemisphere) of 2DG incorporation in cortical layer IV presented as a percentage. According to ANOVA test, the 2DG incorporation was significantly lower in treated (right) hemispheres in **SD** group (p=0.006) by 7% and in the post-stroke **Pt** group (p=0.03) by 13%.

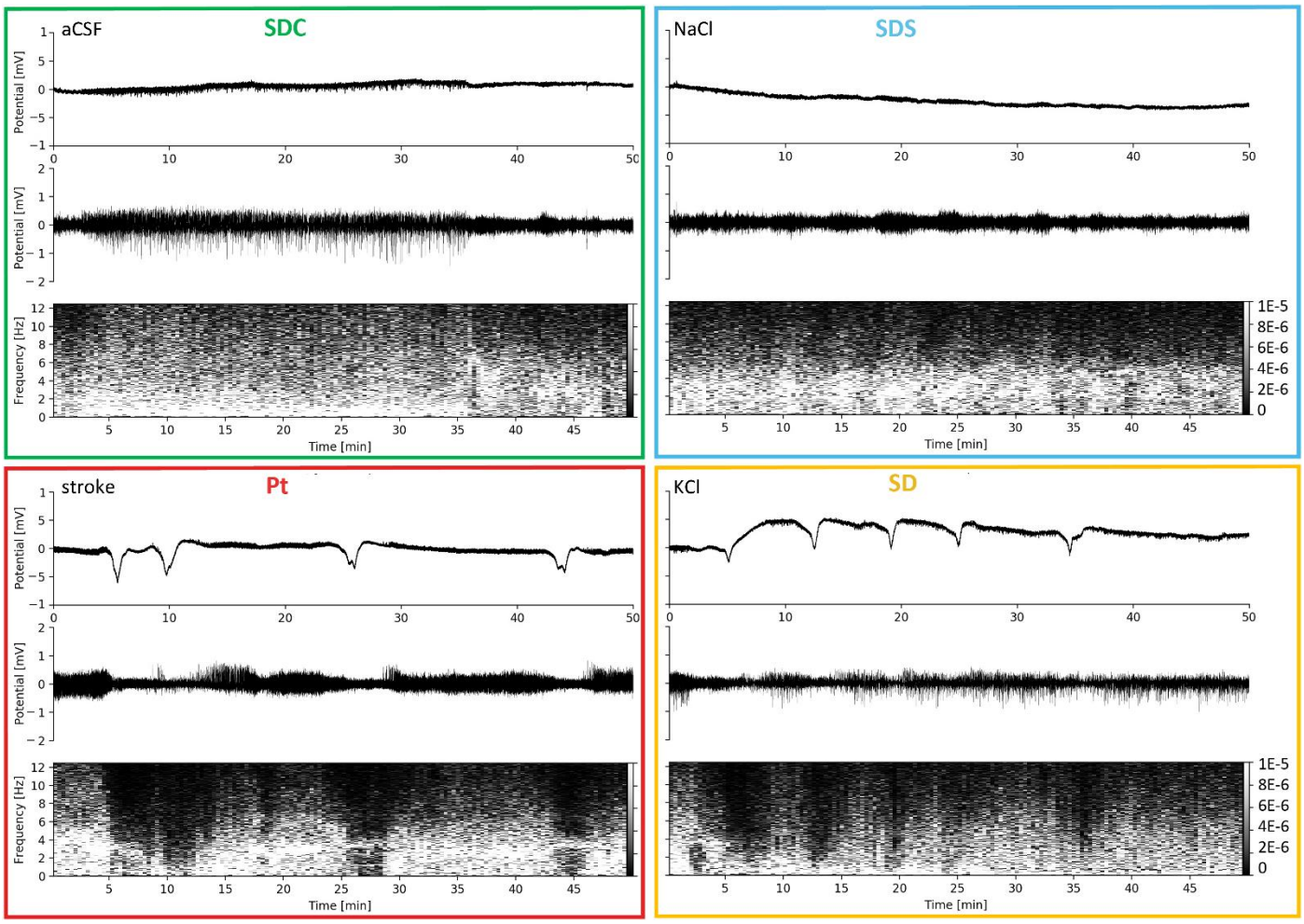


**Fig. 6.** Example plots of recordings for spreading depolarizations. Top pictures present raw ECoG signal. Signals in the middle pictures were filtered 0.1 – 100 Hz with Butterworth 3 rd order filter. Bottom panels present spectrograms computed from the filtered signal (See in methods - DaSt: Electrophysiological statistic). We observe a significant reduction of broad range (4-12 Hz) of ECoG oscillations that correlates with depolarization event both in Pt and SD experimental conditions. SDC (with aCSF) (A), SDS after 3M NaCl application (B), Pt during and after PtS (C) and 3M KCl in SD group (D), (Supp. Fig. 1, 2);

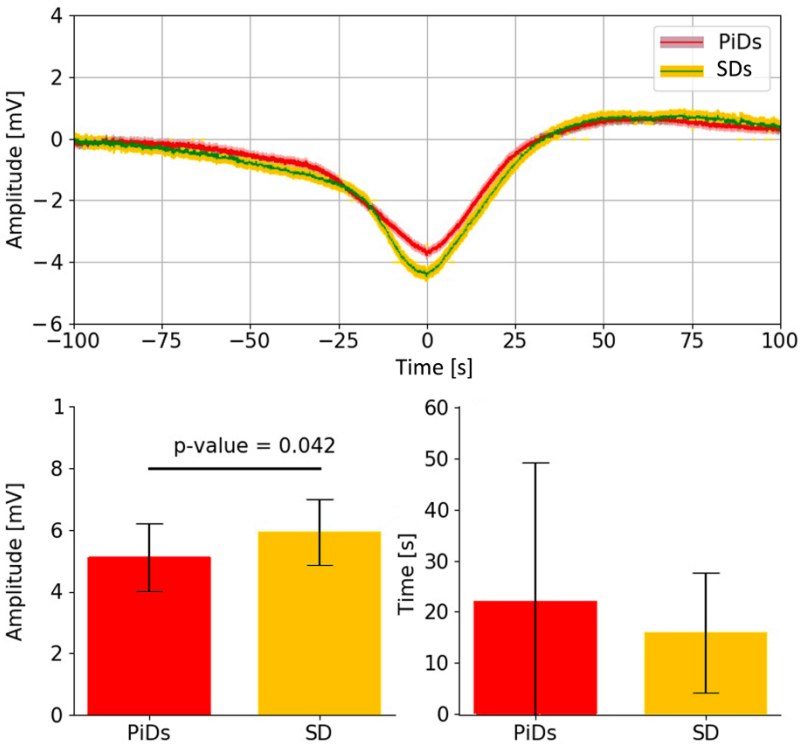


**Fig. 7**. Comparison of the mean events of the depolarizations evoked by KCl application (yellow line) or poststroke PiDs (red line). Top panel presents the mean signal of detrended depolarizations (baseline translated to 0 amplitude). Left bottom picture: compared shape of amplitudes between PiDs and KCl and the found minor difference in total amplitude (from trough to peak of depolarization). Right bottom picture: shows no difference in the time duration of spreading depolarization. The statistic was computed using the resampling method (Supp. Fig. 6-1).

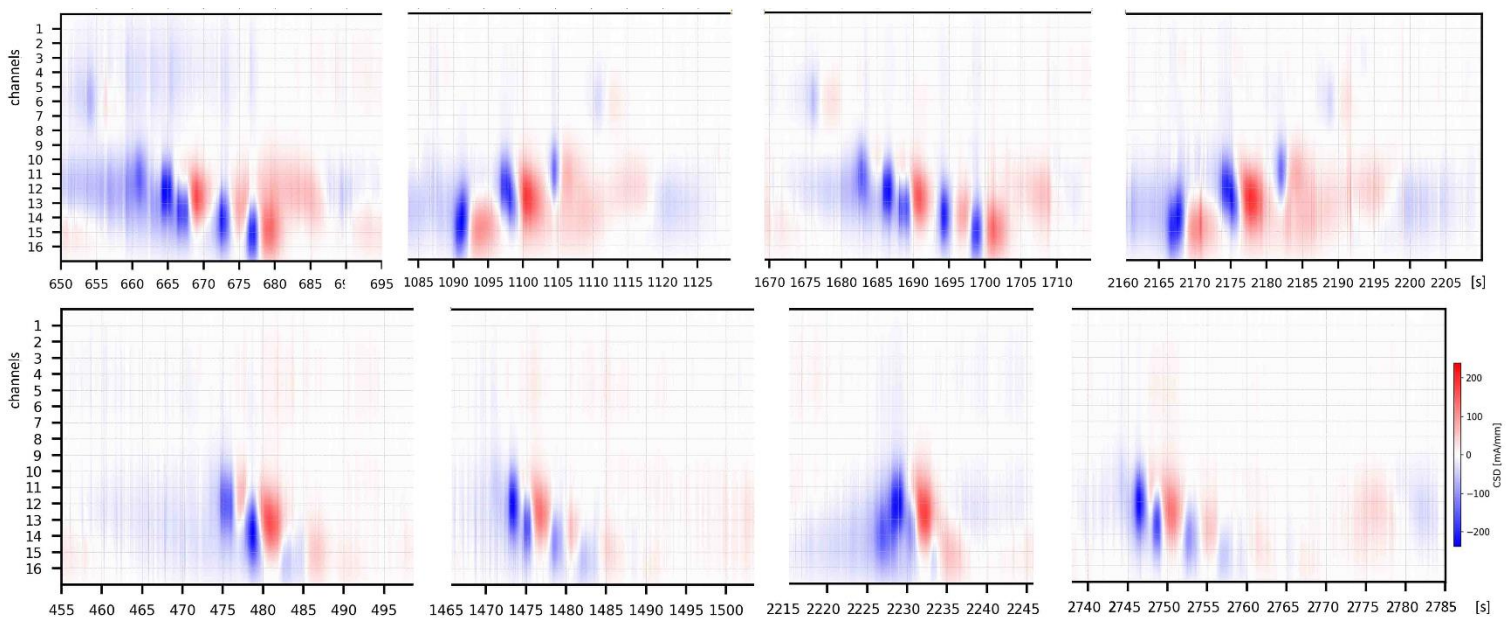


**Fig. 8.** Spreading of the spreading waves of **SD** showed with CSD spectrograms. CSD analysis of example spreading depolarization events evoked with KCl application. Using kCSD analysis we reconstructed current sources and sinks along electrode positions. We assumed constant tissue conductivity for computational purposes (See in methods - DaSt: Multielectrode recordings). The strongest source was in a position from where the wave came and as we present it may cross the monitored area in a few different directions (Supp. Fig. 2).

**Proteins localisation in the:**

**A. barrel field**

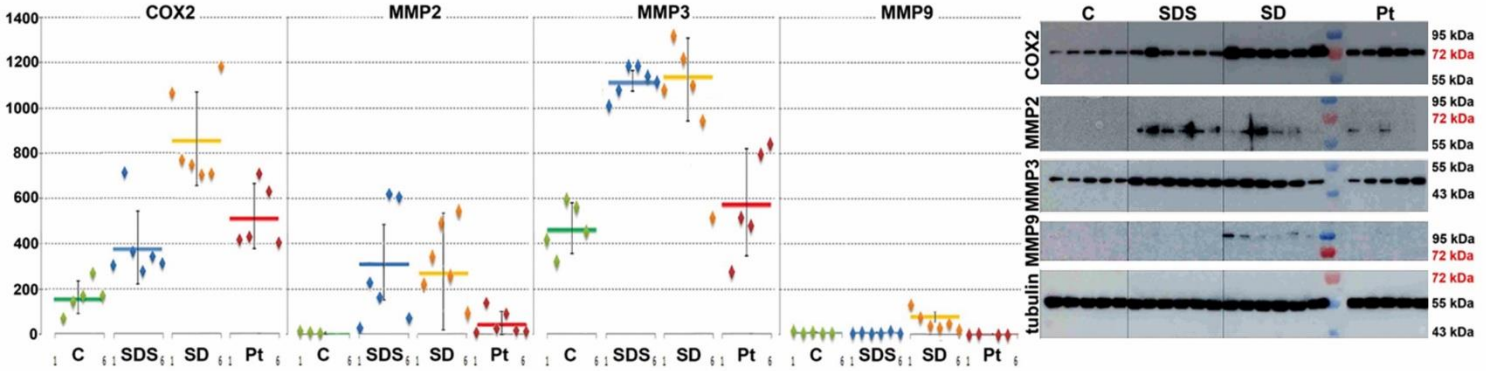


**B. place of solutions application in SD and SDS animals (*sol*)**

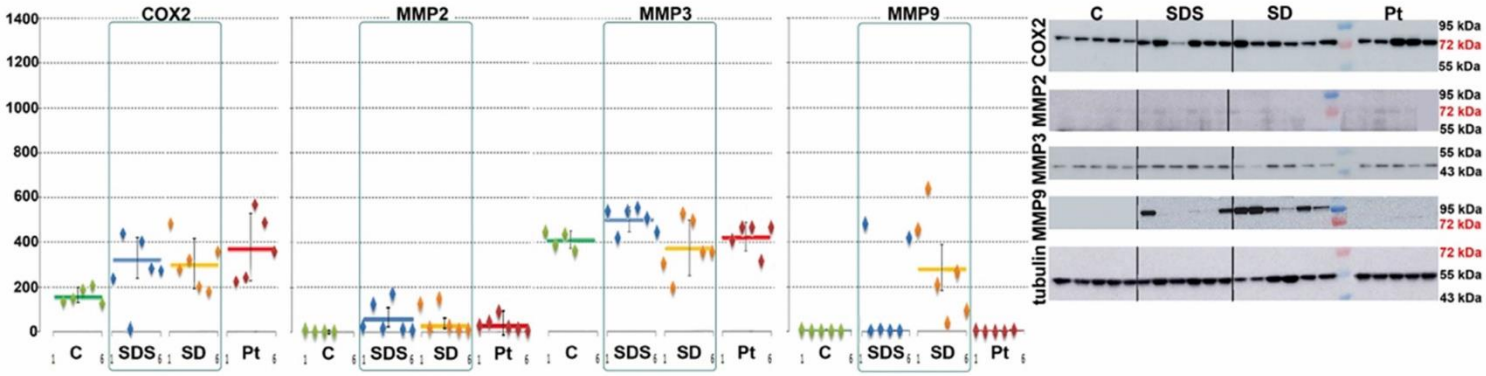


**C. position of the stroke induction in Pt animals (*s*)**

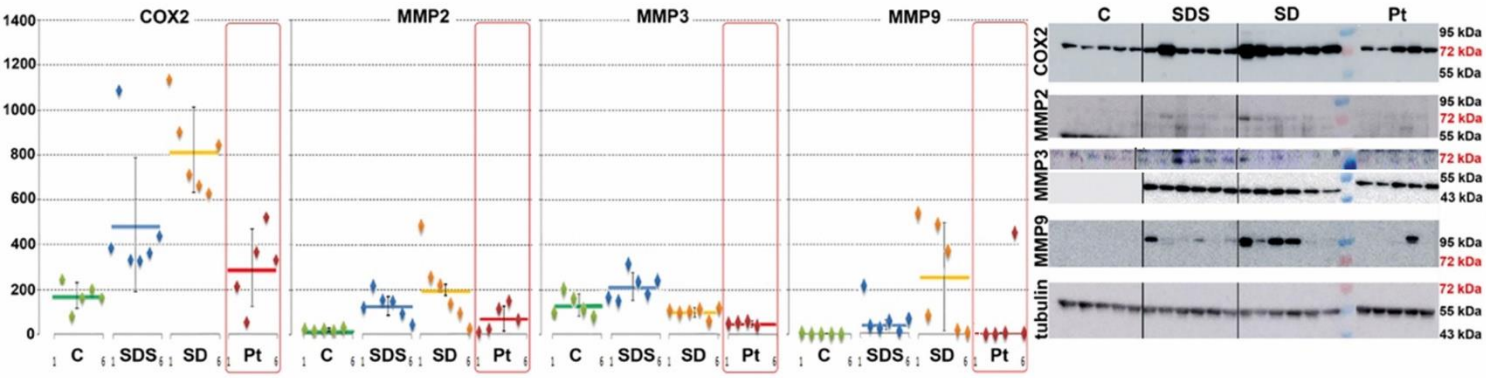


**D. thalamus**

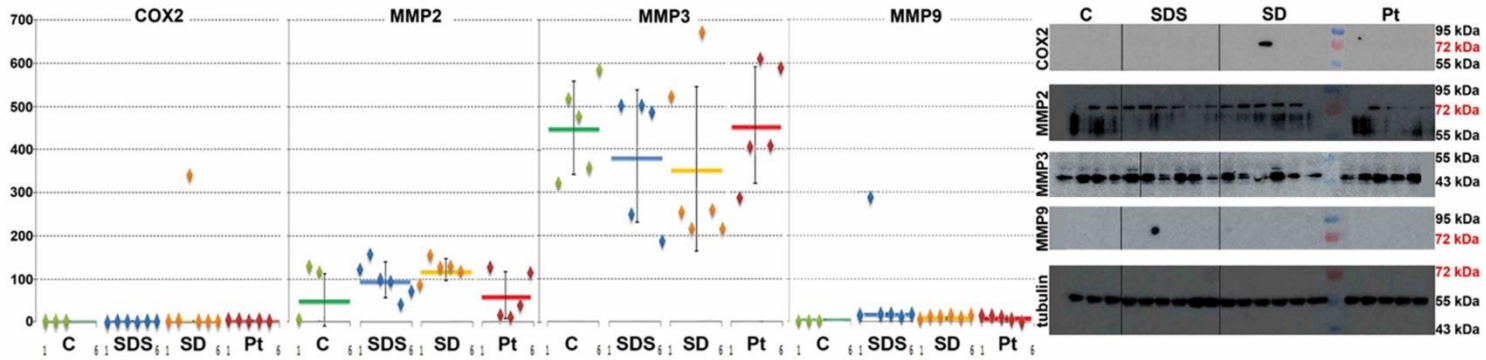

**Fig. 9.** Barrel field concentration of chosen proteins by Western blots of tissue samples from the right hemispheres, the treated in experimental animals: COX - 2, MMP - 2, - 3 and - 9, Diamonds represent results from individual animals, bar — mean of results for each group. On the right, parts of Western blots photos corresponding to the results showed on the graphs. In addition, on the bottom a part of Western blot for tubulin, which was used for normalization. Molecular weight as indicated by molecular weight marker (Supp. Fig. 5).

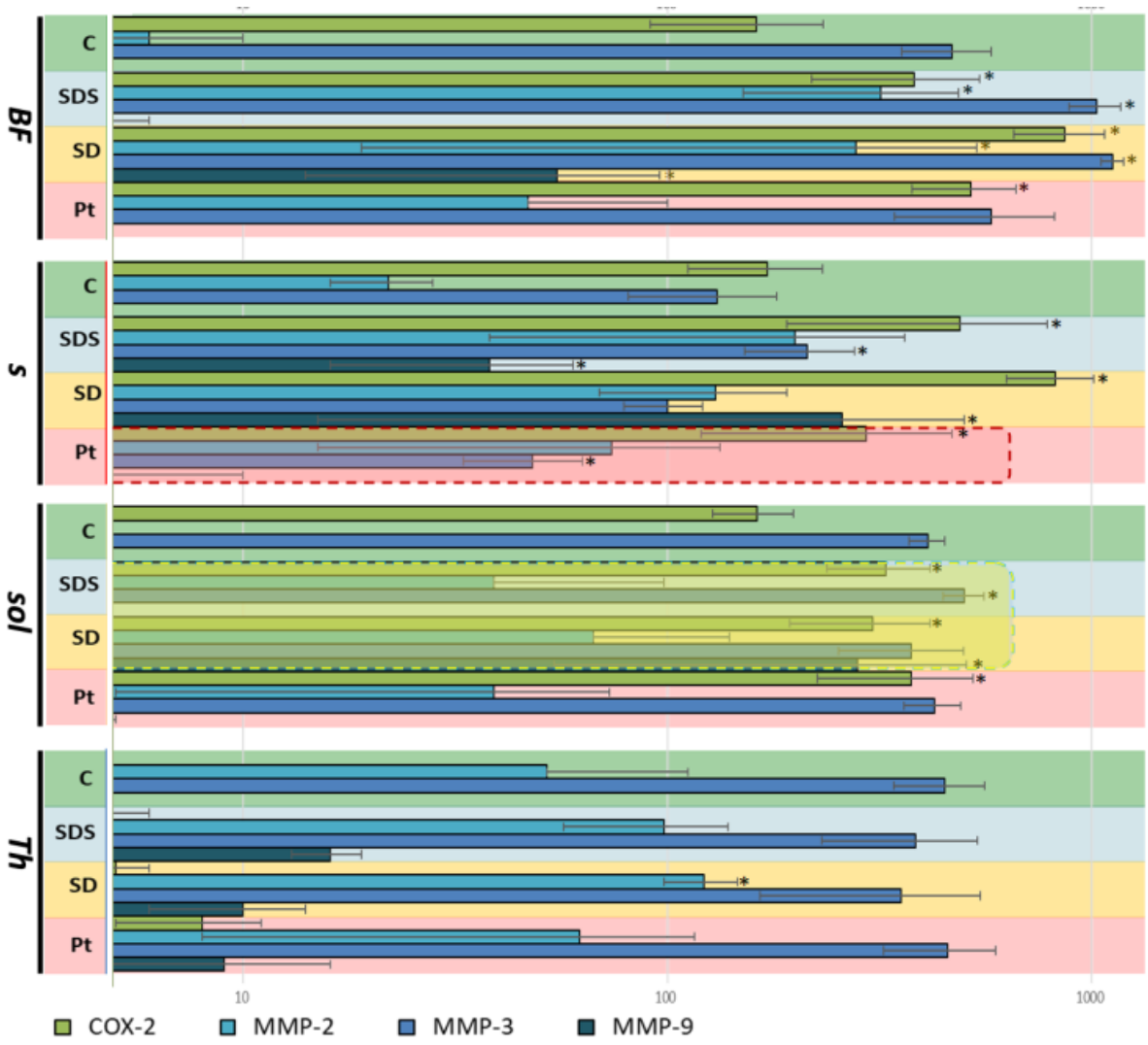


**Fig. 10.** Concentration of chosen proteins by Western blots conducted to, from the left: COX - 2, MMP - 2, - 3 and - 9. Diamonds represent results from individual animals, bar — mean of results for each group. On the right, parts of Western blots photos corresponding to the results showed on the graphs. In addition, on the bottom a part of Western blot for tubulin, which was used for normalization. Molecular weight as indicated by molecular weight marker (Supp. Fig. 5)

**Supp.1**

Experience dependent plasticity (I)

One month unilateral deprivation of all but one row of whiskers resulted in non-deprived rows widening in all experimental and control groups [Fig. 2 & 3]:

- **C:** in control group deprivation resulted in 42% ± 14% widening of non-deprived row B cortical sensory representation in hemisphere contralateral to the deprived whiskers (1160 ± 121 μm) in comparison to the same row in non-deprived hemisphere (814 ± 15 μm; p = 0.009);
- **Pt:** after stroke the deprivation resulted in 11% ± 9% widening of non-deprived row B cortical sensory representation (906 ± 76 μm to 821 ± 113 μm; p = 0.017);
- **SDC:** in aCSF treated group deprivation resulted in 35% ± 27% non-deprived row cortical sensory representation widening (1075 ± 132 μm) in comparison to the same row in non-deprived hemisphere (798 ± 108 μm; p = 0.03);
- **SDS:** in the sham group, 3M NaCl application resulted in small lesion in occipital cortex. The difference in the width between rows B representations of the deprived (1023 ± 192 μm) and non-deprived (779 ± 123 μm) hemispheres was 33% ± 26%, p = 0.04;
- **SD:** in animals with spreading depolarisations and the focal lesion induced by 3M KCl the difference between rows B representations was significantly as wall (p <0.001) as in **SDS** and **SDC** groups. However, the mean percentage difference between deprived and non-deprived sites was 42 % ± 18% like in intact control group C; (1036 ± 192 μm in deprived hemisphere vs. 781 ± 81 μm in non-deprived; p = 0.002).

Stroke group was the only one which differed significantly from others when the widening was compared (interhemispheric difference of the rows B representations width 11% to: 42% in **C** , p=0.002; 35% in **SDC**, p=0.009; 33% in **SDS**, p=0.004 and 42% in **SD**, p=0,006). The non-deprived row B representation itself in the deprived hemisphere with focal PtS in the **Pt** animals differed significantly from homologus areas in other groups: **SD** (p=0.006), **C** (p=0.003) and **SDC** (p=0.04). There were no statistically important differences between SD-operated groups in the non-deprived row B cortical representations [Fig. 3].

Regarding this comparisons the **SDS** non-deprived row B representation differed from that of **C** animals (p=0.02), but it is obvious that lack of confirmed difference between the groups in interhemispheric relation allows us to treat it as accidental situation due to one animal in **SDS** group which had the representations thinner in both hemispheres (539 μm vs 859 μm), therefore it will be not discussed later.

**Supp. 2:**

Thalamic changes in all groups were less pronounced, and COX-2 (bands 72 kDa) were not observed. However, an epitope on bands around 180kDa was detected with the highest concentration in four out of six animals of the **SD** group (86±24). Two animals from **Pt** group demonstrated the equivalent level of these bands in the ***th*** (61±19), but again, the other animals did not. Conversely, the **SDS** animals had a relatively low deviation (PD=45%), although the level of the bands OD had a much lower threshold (21±14). We assumed that it was a procedural artifact; nonetheless, the **SD** had a significantly higher density of COX-2 (180kDa, 63±40 vs. **C** 6±6, p=0.02 vs. sham 21±13, p=0.04) and shams had a significantly higher concentration in that band than **C** (p=0.04).

**Supp. 3:**

Nevertheless, one of **C** animals had MMP-2 zymogen detected and two had the mysterious 45kDa epitope which was present in the other experimental groups. The 45kDa epitope was shown to be specific for different anti-MMP-2 antibodies (Novus Biotechnology MMP-2; 43 kDa, cat number - NBP2-37426). Significantly higher concentration of the 45kDa epitope was detected in three animals after stroke (323±24 [An] while in all the other animals in all the experimental groups the concentration was 198±56, p=0.0009).

**Supp. 3:**

MMP-9 in the **C** animals were not detected neither in the thalamus nor in the cortex. MMP-9 in the thalamus was present just in one **SDS** animal, the same animal that had higher MMP-2 thalamic level (157 [An] vs. 97±40 [An] in the rest of the SDS) and was one of the two animals that had lower MMP-3 (248 [An] vs. 496±9 [An] for the rest three of SDS).

**Supp. 4:**

The decrease of MMP-3 synthesis in the stroke core could not be due to the lesion because the ***sol*** region had no defined decrease in the **SD** and in **SDS** it had even a tendency to grow. However, it is still unlikely influencing ExDp in BF.

## Supplementary Figures

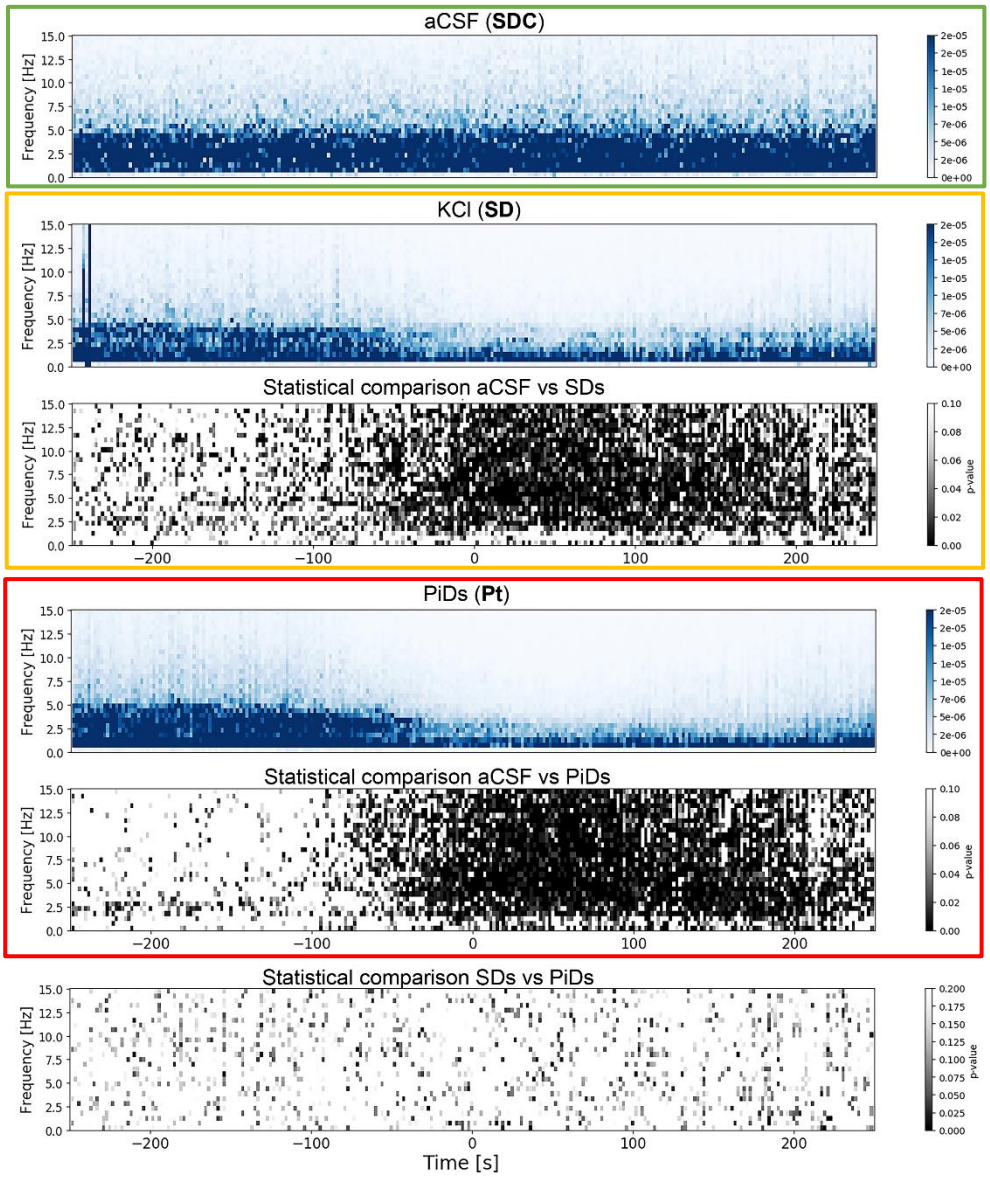


**Supp. Fig. 1: The ECoGs spectrogram** matrices (blue) and statistical comparison (black) between baseline, aCSF treated, **SDC** animals (green frame), SDs of **SD** animals (orange frame) and PiDs of **Pt** (red frame). Timeline is related to through of single SD event (timepoint 0 – minimal voltage value; ±200 [s]). The estimation of differences significance between groups was calculated using resampling method. (See in methods - DaSt: Electrophysiological statistic). Every square represent p-value for difference between means for new random sets of fragments and original difference between two groups (the gray scale of the spectrograms). During depolarization wave there was a significant difference between baseline of **SD** and **Pt** versus **SDC** (p=0.03) There was a significant reduction of 2-12 Hz oscillations during depolarization both for SDs and PiDs but PiDs and SDs did not differ from each other. Most probably spreading depolarizations causes sedation of the large cell populations.

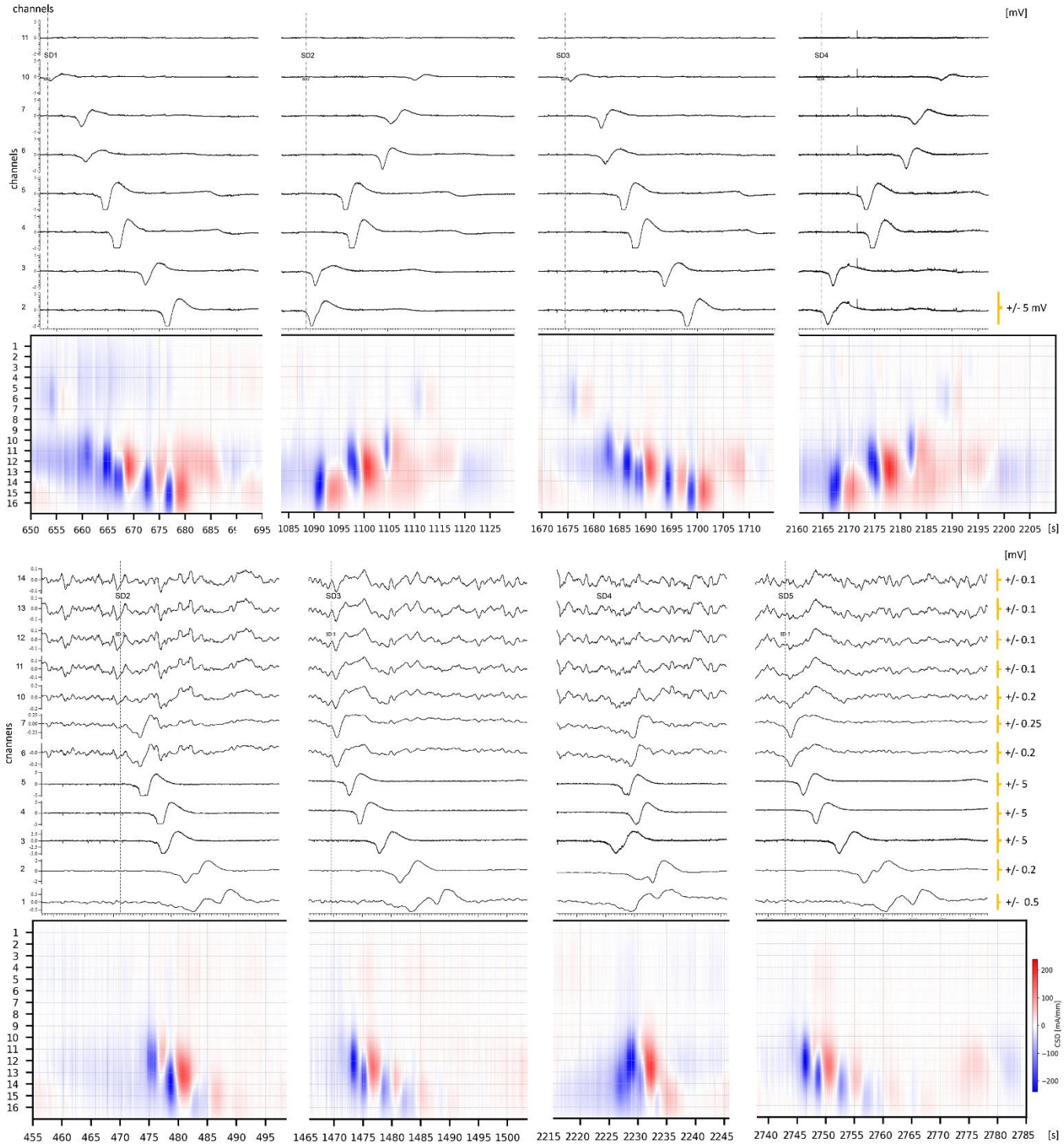


**Supp. Fig. 2: Spreading of the spreading waves & CSD for the examples of chosen spreading waves of SDs**. LFP and CSD analysis of example spreading depolarization events evoked with KCl application in two different animals. Using kCSD analysis we reconstructed current sources and sinks along electrode positions (See in methods - DaSt: Electrophysiological statistic). We assumed constant tissue conductivity for computational purposes. The strongest source was in a position from where the wave came. As we can be seen it crossed the monitored area in few different directions during the same.

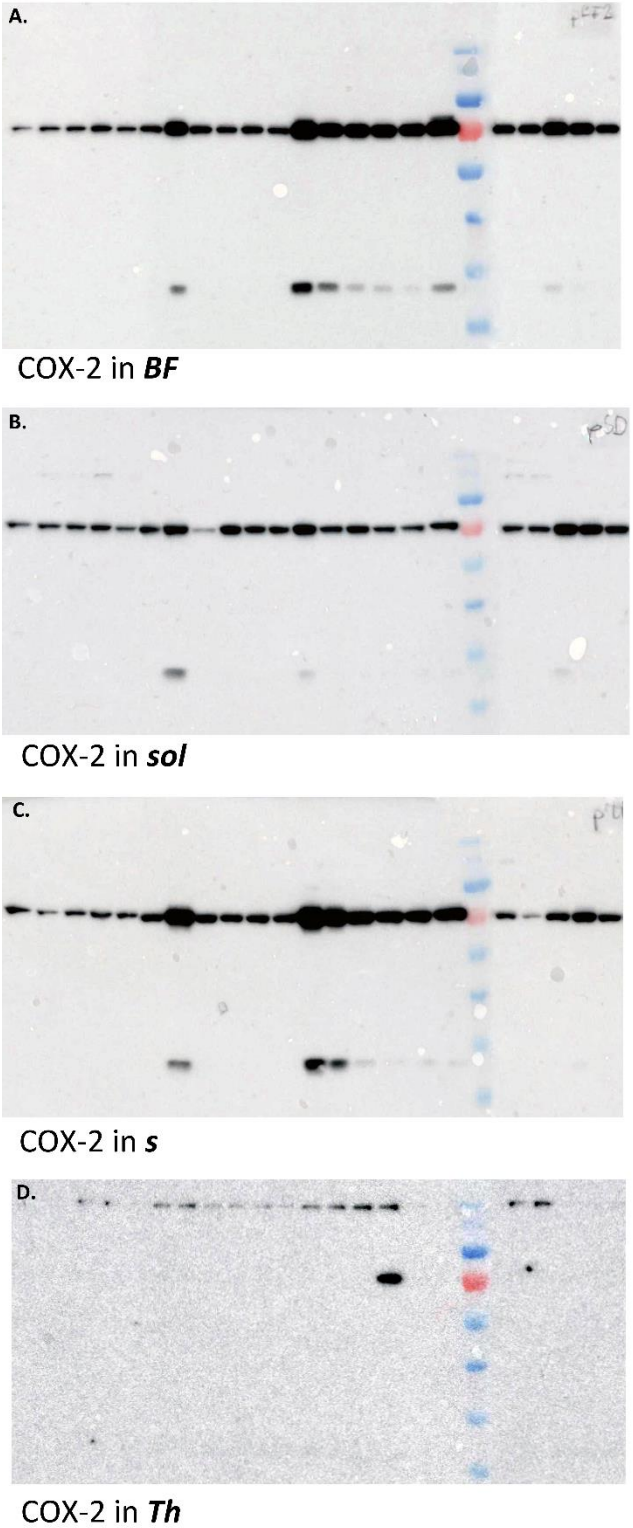


**Supp. Fig. 3: Photos of entire images of Western blot membranes** with protein lysates from brain tissue samples incubated against COX-2. In the cortical areas of (A) barrel fields, (B) the place of solution application, (C) the position of the stroke induction and (D) thalamus with visible additional bands. The protein degradation product (33kDa) can be seen related to the higher concentration of COX-2 within the specimen. In the thalamus series of bands at the weight of 180 kDa are the only presented for the whole animal series. Molecular weight according to molecular weight marker

.

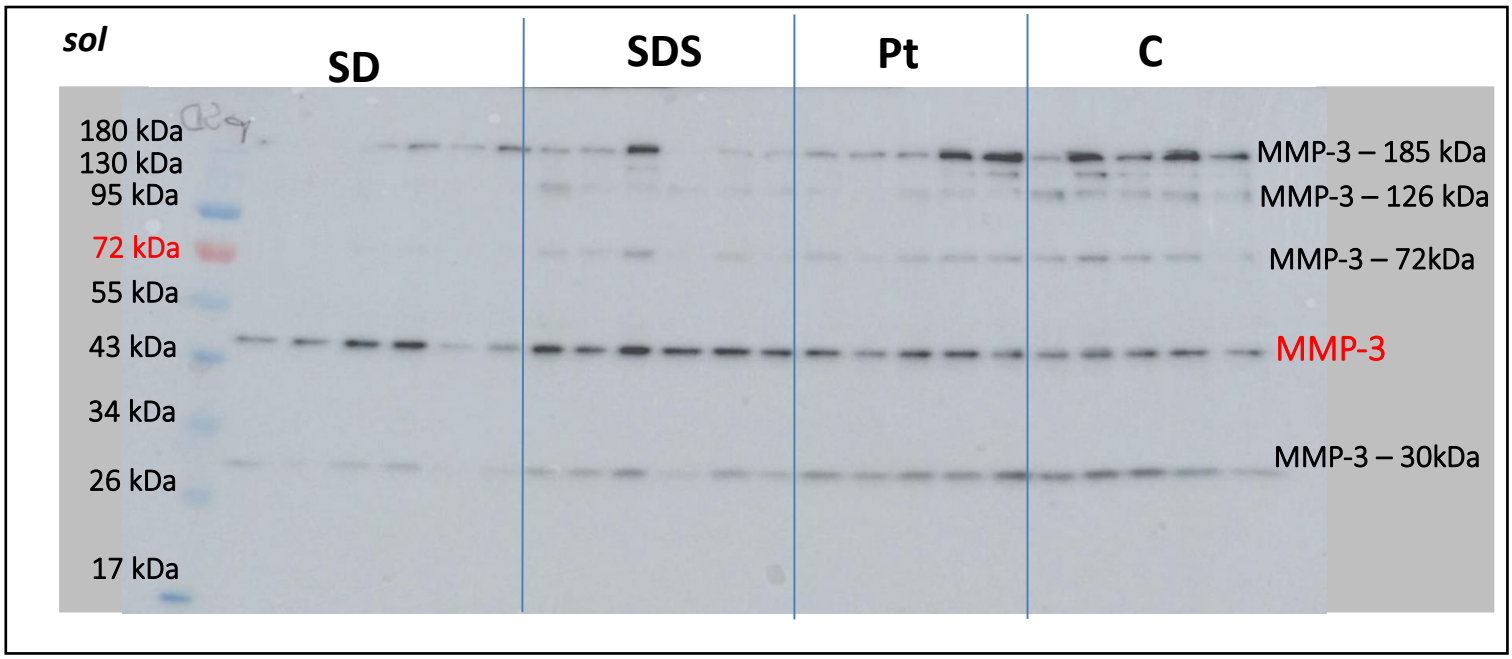


**Supp. Fig. 4: Photos of entire images of Western blot membranes** with protein lysates from brain tissue samples incubated against MMP-3. In the cortical area of solution application in SD-operated animals with visible additional bands. The protein degradation product (30kDa) can be seen related to the lower concentration of MMP-3 in the group of **SD** animals. Molecular weight according to molecular weight marker

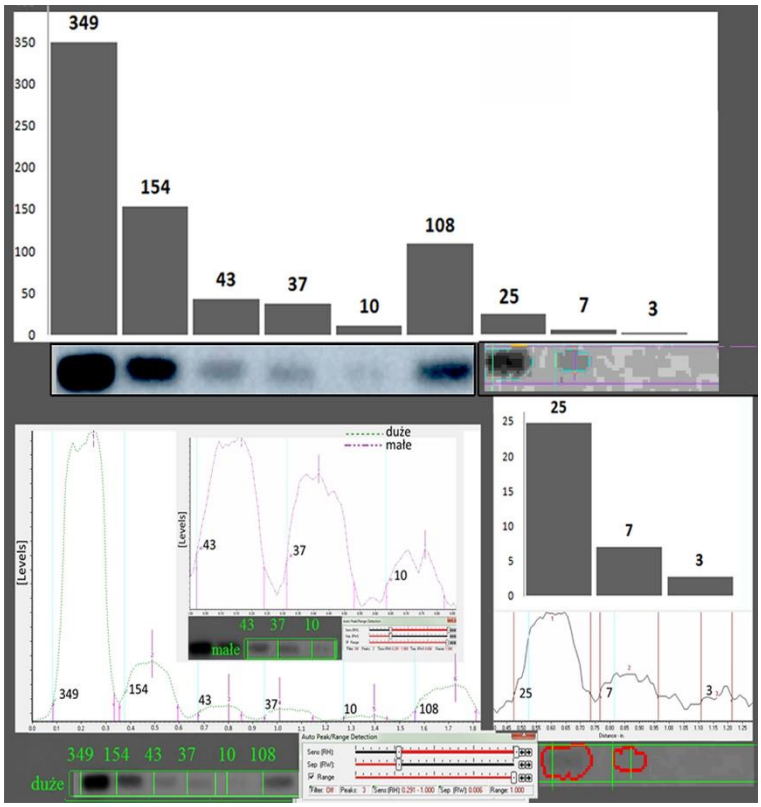


**Supp. Fig. 5: Methodological graph of Western blot analysis** showing the data acquisition procedure, the reference bands of protein different concentration and the relative abstract number [An] used in the text (respective values of OD multiplied by band surface and divided by reference housing protein multiplied by 1000). Below the representative line analysis from the MCID program designed for electrophoresis with "pick detection" and "smiling correction". The series of bands on a bottom with OD and measurement of bands areas.

## Tables

**Supp. Tab. 1: Distribution of animals between experimental groups** (**C**, **Pt**, **SD**, **SDS**, **SDC**). Animals undergoing procedural sets of operations and experimental methods used for monitoring of defined results (**I**- cortical plasticity, **II**- metabolic basis of activity, **III**- electrophysiological basis of activity and spreading waves characteristics, **IV**- protein changes).

| procedures \ groups of animals | | | C | | Pt | SD-operated | | |
|---|---|---|---|---|---|---|---|---|
| | | | | | | SD | SDS | SDC |
| | | | intact | | stroke operation | SD-like operation | | |
| methods | | treatment results | | | BR and light | 3M KCl | 3M NaCl | aCSF |
| I. | 2-DG brain mapping | cortical plasticity | n =6 **a: I, II** | whiskers deprivation n=6 **b: I, II** | n=6 **e: I, II** | n=8 **c: I, I,IIIA** | n=5 **d: I, II,IIIA** | n=5 **a: I, II,IIIA** |
| II. | | metabolic basis of activity | | | | | | |
| III. | ECoG | spreading waves | | | n=6 **IIIA** | | | |
| | | spontaneous activity | | | | | | |
| IV. | Western blots | COX-2 | n=5 **IV** | | n=5 **IV** | n=6 **IIIB, IV** | n=6 **IIIB, IV** | |
| | | MMP-2 | | | | | | |
| | | MMP-3 | | | | | | |
| | | MMP-9 | | | | | | |
| | | Tubulin | | | | | | |
| | | GAPDH | | | | | | |

| Groups | Stimulated row of whiskers representation width [µm] | | interhemispheric difference [%] | Significance of the difference |
|---|---|---|---|---|
| | Hemisphere | | | |
| | **undeprived** | **deprived** | | |
| **C** | 814 ± 15 | 1160 ± 121 | 42 ± 14 | p = 0.009 |
| **Pt** | 821 ± 113 | 906±76 | 11 ± 9 | p = 0.02 |
| **SDC** | 798 ± 108 | 1075±132 | 35 ± 27 | p = 0.03 |
| **SDS** | 779 ± 123 | 1023±192 | 33 ± 26 | p = 0.04 |
| **SD** | 781 ± 81 | 1036±192 | 42 ± 18 | p = 0.002 |

**Tab. 2:** Non-deprived row B cortical representation width with percentage of interhemispheric difference and its significance; p<0.05

**A.**

| Groups | 2DG incorporation in cortical rows B representations [µCi/g] | | interhemispheric difference of 2DG incorporation in cortical rows B representations | significance of the inter-hemispheric difference |
|---|---|---|---|---|
| | hemisphere | | | |
| | **intact** | **treated** | | |
| **C** | 1.08 ± 0.1 | 1.08 ± 0.1 | 1 ± 0.1 | |
| **Pt** | 1.17 ± 0.2 | 1.13 ± 0.1 | 0.96 ± 0.04 | |
| **SDC** | 1.03 ± 0.3 | 1.16 ± 0.4 | 1.05 ± 0.08 | |
| **SDS** | 1.28 ± 0.6 | 1.32 ± 0.6 | 1.04 ± 0.1 | |
| **SD** | 1.23 ± 0.1 | 1.13 ± 0.2 | 1.08 ± 0.5 | 8% |

**B.**

| Groups | 2DG incorporation on entire sections of hemispheres [µCi/g] | | interhemispheric difference of entire sections 2DG incorporation | significance of the inter-hemispheric difference |
|---|---|---|---|---|
| | hemisphere | | | |
| | **intact** | **treated** | | |
| **C** | 1.02 ± 0.2 | 1.04 ± 0.2 | 1.02 ± 0.04 | |
| **Pt** | 1.19 ± 0.04 | 1.03 ± 0.1 | 1.13 ± 0.08 | 13% |
| **SDC** | 0.99 ± 0.2 | 1.02 ± 0.3 | 1.03 ± 0.06 | |
| **SDS** | 1.09 ± 0.4 | 1.09 ± 0.5 | 1.00 ± 0.04 | |
| **SD** | 1.06 ± 0.2 | 1.02 ± 0.2 | 1.07 ± 0.09 | 7% |

**Tab.3**: 2DG incorporation [µCi/g] in cortical rows B representations (A.) and on entire sections of the intact and treated hemispheres (B.) with the percentage of the significant differences; p<0.05.

| protein | COX-2 (72kDa) | | | | MMP-2 (64kDa) | | | | MMP-3 (48kDa) | | | | MMP-9 (95kDa) | | | |
|---|---|---|---|---|---|---|---|---|---|---|---|---|---|---|---|---|
| area\group | C | SDS | SD | Pt | C | SDS | SD | Pt | C | SDS | SD | Pt | C | SDS | SD | Pt |
| BF | 162 | 382 | 864 | 520 | 6 | 318 | 278 | 47 | 468 | 1028 | 1120 | 581 | 0 | 2 | 55 | 0 |
| | *71* | *163* | *208* | *143* | *4* | *167* | *259* | *53* | *111* | *143* | *69* | *238* | *5* | *4* | *41* | *1* |
| | $F_{(3,18)}$ = 19.33, p <0.0001) | | | | $F_{(3,17)}$ = 4.26, p = 0.02 | | | | $F_{(3,18)}$ = 14.65, p<0.0001 | | | | $F_{(3,16)}$ = 7.62, p = 0.002 | | | |
| | p = | 0.02 | 0.0002 | 0.002 | p = | 0.05 | 0.006 | 0.01 | p = | <0.0001 | <0.0001 | 0.01 | p = | >> | <0.0001 | >> |
| *s* | 172 | 489 | 822 | 294 | 22 | 200 | 112 | 74 | 131 | 214 | 100 | 48 | 1 | 38 | 258 | 4 |
| | *60* | *298* | *191* | *174* | *6* | *162* | *43* | *59* | *50* | *62* | *21* | *15* | *3* | *22* | *243* | *6* |
| | $F_{(3,18)}$ = 10.6, p <0.001 | | | | $F_{(3,18)}$ = 7.32, p=0.003 | | | | $F_{(3,18)}$=13.01, p <0.0001 | | | | $F_{(3,16)}$=6.25, p=0.006 | | | |
| | p = | 0.04 | 0.0002 | | p = | | 0.004 | | p = | 0.04 | | 0.02 | p = | 0.02 | 0.05 | |
| *sol* | 163 | 327 | 305 | 376 | 1 | 39 | 67 | 54 | 411 | 502 | 376 | 426 | 0 | 2 | 281 | 3 |
| | *35* | *89* | *111* | *150* | *1* | *59* | *73* | *31* | *39* | *55* | *123* | *65* | *5* | *2* | *227* | *2* |
| | $F_{(3,17)}$ = 3.78, p =0.03 | | | | $F_{(3,18)}$ = 7.32, p=0.003 | | | | $F_{(3,18)}$=2.54, p=0.09 | | | | $F_{(3,15)}$=6.25, p=0.017 | | | |
| | p = | 0.01 | 0.02 | 0.03 | p = | | | 0.008 | p = | 0.02 | | | p = | | 0.03 | |
| Th | 2 | 4 | 5 | 8 | 52 | 98 | 122 | 62 | 451 | 385 | 356 | 458 | 0 | 16 | 10 | 9 |
| | *1* | *2* | *1* | *3* | *60* | *41* | *24* | *54* | *109* | *154* | *191* | *135* | *2* | *3* | *4* | *7* |
| *cortical PD* | *3* | *17* | *4* | *23* | *114* | *32* | *51* | *13* | *54* | *93* | *118* | *22* | *118* | *124* | *91* | *163* |

**Tab. 4:** Protein amounts in abstract numbers [An] with *SD* below (An of a band OD - OD of the reference housekeeping protein [levels] x area [um]). Values significantly different from control have a red font; $p < 0.05$. Percentage deviations of cortical proteins amount on the table bottom show that metalloproteinases had ten times higher deviation than COX-2 in the intact brains and from 3 to 7 times higher postoperative intracortical deviations. Green background marks the control values. The injured areas are marked with colour backgrounds (yellow – the highly osmotic solution application, red – the illuminated area injured by the PtS).